Mathematical Tripos Part III
Essay

Anomalous Muon Magnetic Moment and Lattice QCD

Department of Applied Mathematics and Theoretical Physics
University of Cambridge

Contents

1 Introduction

The anomalous muon magnetic moment, a_μ, is an additional contribution to the lepton's magnetic moment due to loop corrections. This deviation from the magnetic moment predicted by Dirac's theory can be defined as [1]

$$a_\mu = \frac{g-2}{2}, \tag{1.1}$$

where g is the Landé g-factor.

The anomalous muon magnetic moment receives contributions from all sectors of the Standard Model. To make this point manifest, we can split a_μ based on the contributing sectors [2],

$$a_\mu^{\mathrm{SM}} = a_\mu^{\mathrm{QED}} + a_\mu^{\mathrm{EW}} + a_\mu^{\mathrm{had}}, \tag{1.2}$$

corresponding to radiative corrections due to virtual leptons and photons, gauge bosons and hadrons respectively. As a consequence, performing a precision measurement on a_μ allows us to probe for new physics since any coupling of the muon to undiscovered particles, be it through Standard Model interactions or beyond, will contribute to the anomalous magnetic moment [3]. Thus, any discrepancies found between the measured a_μ and the Standard Model prediction could provide hints of interactions that are unaccounted for in the theory.

In this literature review, we will first acquaint ourselves with the origin of the anomalous magnetic muon. This is followed by a review of the measurements made in the Brookhaven National Laboratory (BNL) during the E821 experiment. The main section of the review will be devoted to studying the methods used in evaluating hadronic contributions to the anomalous muon magnetic moment. The low energy regime of Quantum Chromodynamics (QCD) is non-perturbative. Thus, we rely on ever-improving numerical techniques developed in the vibrant field of Lattice Quantum Chromodynamics.

2 g-2: A Brief History

Here the origin of the anomalous magnetic moment is presented in a brief historical narration. A more detailed account of the history on g-2 can be found in the review by Miller, de Rafael and Roberts [4].

Experiments such as those performed by Stern and Gerlach in 1922 and Phipps and Taylor in 1927 revealed that the magnetic moment of the atoms in the presence of a non-uniform magnetic field are split into two bands, representing two discrete values for the z-component of the magnetic moment [5]. The interpretation given by Uhlenbeck and Goudsmit was that the unpaired electron in both the silver atoms (Stern & Gerlach) and the hydrogen beam (Phipps & Taylor) has an intrinsic angular momentum built in. This angular momentum, now known as the *spin* angular momentum, is quantum in nature and is responsible for the discrete values of the magnetic moment.

The magnetic moment, $\vec{\mu}$, of a charged particle has the following form [2]

$$\vec{\mu} = g\frac{q}{2m}\vec{S}, \tag{2.1}$$

where q and m are the charge and mass of the particle respectively, g is the Landé g-factor and $\vec{S}$ is the spin angular momentum. The two bands observed in the experiments correspond to the fact that the electrons are spin-1/2 particles. Thus, the z-component of the spin may take on two discrete values, $s_z = \pm\hbar/2$. Using the fact that the experiments measured the z-component of the magnetic moment to be one Bohr magneton, $e\hbar/2m_e$, the Landé g-factor is deduced to be $g = 2$.

In fact, the value of the g-factor was also predicted from Dirac's wave equation for relativistic electrons in 1928. The Klein-Gordon equation of the electron can be manipulated [6] to yield

$$\left(-2im\frac{\partial}{\partial t} - \nabla^2 - e\vec{B}\cdot(\vec{L} + 2\vec{S})\right)\psi = 0. \tag{2.2}$$

The g-factors for the orbital and spin angular momentum are the coefficients that couple to their respective operators, where we see that g=2 emerges naturally for the spin of an electron.

However, in 1947, experimental evidence indicated that the splitting due to the hyperfine structure of the hydrogen is larger than that predicted from the Dirac theory [1]. The insight provided by Schwinger is that this is due to loop corrections to the magnetic moment, where the electron radiates virtual particles in the presence of a magnetic field. To account for this discrepancy, we can split the magnetic moment into two pieces,

$$\mu = (1 + a)\frac{q\hbar}{2m}, \tag{2.3}$$

where the first piece corresponds to the prediction from Dirac's theory and the second piece, a, is defined in Equation 4.34. One can then predict a by computing loop corrections. Although this was originally proposed to resolve the disagreement between measurement and prediction of the electron magnetic moment, we know now that this anomaly is present in both muons and tauons as well. However, for the remainder of this review we will concern ourselves with a_μ and the justification for this will be provided in the beginning paragraph of §4.

3 Experimental Measurements

The value for a_μ has been measured to ever increasing precision in the last 50 years, with the first precision measurement made during the CERN I experiment in 1961 [3] to the more recent E929 experiment in Fermilab that begun taking data in 2017. Since the CERN III experiment in 1974, the general setup for the muon g-2 experiments has been the same, with improvements introduced by

the team in Brookhaven National Laboratory (BNL) in the subsequent decades. The discussion below follows the setup from the E821 experiment from BNL [7].

A beam of protons is accelerated to hit a target. These collisions produce pions, which are steered into a long beamline where they decay into muons and neutrinos. For a process such as $\pi^+ \rightarrow \mu^+\nu_\mu$, the high energy muons are selected. This selection criteria corresponds to muons which decay in the direction of the original pion's trajcetory. The parity violating nature of the weak interaction means that these muons are exclusively left-handed [8]. The polarised beam are then injected into the muon storage ring with cyclotron frequency, ω_c. They remain in orbit under a uniform magnetic field, B, where the spin of the muons precesses with frequency, ω_s.

By measuring the difference between the cyclotron and spin precession frequency, the anomalous muon magnetic moment can be quantified as

$$\vec{\omega}_a \equiv \vec{\omega}_s - \vec{\omega}_c = \frac{e}{m}\left(a_\mu \vec{B} - (a_\mu - \frac{1}{\gamma^2 - 1})\frac{\vec{\beta} \times \vec{E}}{c}\right), \tag{3.1}$$

where e and m are the charge and mass of the muon respectively, $\vec{B}$ is the magnetic field perpendicular to the plane of the muon orbit, $\vec{E}$ is the quadrupole electric field and $\vec{\beta}$ and γ are the usual relativistic beta and Lorentz factor of the muon respectively. The speed of light c was also included to give ω_a the right dimension. By selecting muons with the "magic" momentum, $p_\mu = 3.094\text{GeV/c}$ corresponding to a Lorentz factor of $\gamma \approx 29.3$, to enter the muon storage ring, the electric quadrupole term in Equation 3.1 vanishes. The determination of a_μ amounts to precise measurements of the magnetic field B and the precession frequency, ω_a as the following form suggests

$$\omega_a = a_\mu \frac{eB}{m}. \tag{3.2}$$

The magnetic field can be measured in terms of the NMR frequency of the free proton, ω_p. Thus, Equation 3.2 can be rewritten as

$$\begin{aligned} a_\mu &= \frac{\omega_a}{\omega_L - \omega_a}, \\ &= \frac{\omega_a/\omega_p}{\omega_L/\omega_p - \omega_a/\omega_p}, \\ \Rightarrow a_\mu &= \frac{\mathrm{R}}{\lambda - \mathrm{R}}, \end{aligned} \tag{3.3}$$

where ω_L is the Larmor precession of the muon. The muon-to-proton magnetic moment ratio, λ, is determined from the measurement of the Zeeman ground state hyperfine transition of the muonium [9]. Thus, the BNL experiment E821 was tasked to measure the ratio R in order to determine the value of a_μ .

From the precision measurements done by W. Liu et al. [9], the muon-to-proton ratio was determined to be, $\lambda = 3.18334513(39)$, where te uncertainty

quoted is due to statistical errors. The report compiled by G. W. Bennet *et al.* [7] studied the experimental measurements that were conducted through the years between 1999 to 2001. In total, there were two R ratios for μ^+ and one for μ^-, taken from the R99, R00, R01 experiments. By assuming CPT invariance, the average of the three R ratios are

$$\mathrm{R}_\mu^{\mathrm{E821}} = 0.0037072064(20). \tag{3.4}$$

This gives the experimental value of the anomalous magnetic moment [4]

$$a_\mu^{\mathrm{E821}} = 11659208.0(5.4)(3.3) \times 10^{-10}, \tag{3.5}$$

where the statistical and systematic uncertainties are given respectively. With the R01 period finished, the Brookhaven muon g-2 experiments are now formally completed. As mentioned in the opening paragraph of this section, the E929 experiment at Fermilab will aim to further reduce the uncertainties of the a_μ measurement, with the goal of improving the precision by four-fold [3].

4 Theory - Standard Model Predictions

All known charged leptons possess an anomalous magnetic moment. As of 2007, the experimental uncertainty of the muon anomalous magnetic moment is ± 0.05ppm. This is about 770 times larger than that of the electron anomalous magnetic moment [4]. Despite the greater uncertainty, there is a strong theoretical motivation for using the muon as the main probe for new physics. Namely, it is more sensitive to non-QED contributions than the electron. The contribution to the anomalous magnetic moment due to a massive virtual particle, M_X, scales as $(m/M_X)^2$, where m is the mass of the charged lepton. This means that a_μ is $(m_\mu/m_e)^2 \approx 40000$ more sensitive to such contributions than that of a_e [3]. In principle, this would make a_τ the best probe for new physics from the lepton sector. However, due to its much shorter lifetime[1], this poses a formidable challenge for precision measurements in experiments [3].

Since any discrepancy between theoretical prediction and experimental measurement can hint at new physics currently unaccounted for by the Standard Model, it is therefore in our best interest to produce a_μ^{SM} to a precision standard that matches that of experiments. In this section, we will discuss the progress in calculating a_μ^{SM}. We begin by briefly reviewing the successes in obtaining the QED and electroweak contributions. The remainder of this ltierature review will be dedicated to confronting the non-perturbative nature of hadronic contributions.

4.1 QED Contributions

In discussing contributions due to QED processes, we will mainly be following the review produced by Jegerlehner and Nyffeler [1] and the results of Aoyama

[1]For reference, $\tau_\mu = (2.1969811 \pm 0.0000022) \times 10^{-6}$s and $\tau_\tau = (290.3 \pm 0.5) \times 10^{-15}$s [10].

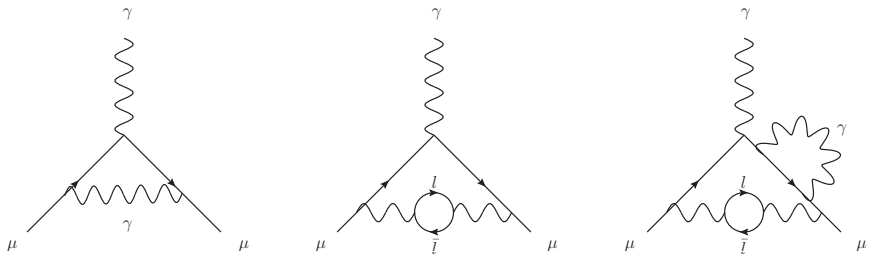

Figure 1: Sample Feynman diagrams depicting QED contributions to the muon anomalous magnetic moment. **Left**: lowest order universal term - the famous Schwinger term. **Centre**: one of 9 second order mass dependent term. **Right**: one of 72 third order mass dependent term. Note that mass dependent terms can become universal terms when $l = \mu$.

et al. [11] A sample of Feynman diagrams involving QED interactions can be found in Figure1.

Historically, contributions from Quantum Electrodynamics to the anomalous magnetic moment of leptons were the first to be accounted for. The famous work by Schwinger [12] determined the first order QED contribution to be $\alpha/2\pi$, where α is the fine structure constant. In principle, the smallness of α allows one to compute arbitrarily high order contributions analytically. Unfortunately, in practice, the number of Feynman diagrams become unmanageable and the amplitudes increasingly difficult to compute. Instead, numerical integrations are employed, for example, from four-loop diagrams onwards [11].

To compute the QED contributions to a_μ^{SM}, we write the QED sector as

$$a_\mu^{\mathrm{QED}} = \sum_{n=1}^{\infty} \left(\frac{\alpha}{\pi}\right)^n a_\mu^{(2n)}, \tag{4.1}$$

where n refers to the n-loop correction. We can further organise the terms of $a_\mu^{(2n)}$ as

$$a_\mu^{(2n)} = A_1^{(2n)} + A_2^{(2n)}\left(\frac{m_\mu}{m_e}\right) + A_2^{(2n)}\left(\frac{m_\mu}{m_\tau}\right) + A_3^{(2n)}\left(\frac{m_\mu}{m_e}, \frac{m_\mu}{m_\tau}\right), \tag{4.2}$$

where $A_1^{(2n)}$ are the mass independent (universal) contributions and $A_2^{(2n)}$ are the mass dependent terms. We note that for $n = 2, 3$, the contributions are known analytically. For $n \gtrsim 4$, Aoyama *et al.* resorted to numerical integration, as stated above.

It is clear from Equation 4.1 that a precise prediction of a_μ^{QED} requires precise knowledge of the lepton mass ratios and the fine structure constant. For the former, Aoyama referred to the values provided by CODATA [13], namely $m_\mu/m_e = 206.7682843(52)$ and $m_\mu/m_\tau = 5.94649(54) \times 10^{-2}$. As for the latter, two different approaches were used to obtain α: one by the precisely measured

Rydberg constant (denoted Rb below) and the other via the anomalous magnetic moment of the electron.

Below, we quote the QED contributions to a_μ^{SM} up to the $n = 5$-loop correction, using two different determinations of α:

$$\begin{aligned} a_\mu^{\mathrm{QED}}(\mathrm{Rb}) &= 116584718951(9)(19)(7)(77) \times 10^{-14}, \\ a_\mu^{\mathrm{QED}}(a_e) &= 116584718846(9)(19)(7)(30) \times 10^{-14} \end{aligned} \tag{4.3}$$

where the uncertainties are due to the lepton mass ratios, the 4- and 5-loop correction terms and α_e respectively.

As we will see in subsequent sections, a_μ^{QED} contributes the most to a_μ^{SM} out of all the other terms in Equation 1.2. Thus, it remains an important effort to further reduce the uncertainties in Equation 4.3 and to strive for higher loop terms.

4.2 Electroweak Contributions

In this section, we will follow the progress made by Gnendiger *et al.* [14]. For details regarding the parametrisation used in determining the W mass, and subsequently α_μ^{EW}, we refer to the 2012 particle physics review [15] used in Gnendiger's paper.

After QED processes, the next dominant contribution comes from the electroweak sector. Even so, we see that there exists strong suppression factors of at least $m_\mu^2/M_W^2 \approx 4 \times 10^{-9}$ [2], owing to the massive gause bosons involved in the processes. According to Gnendiger [14], we can organise the electroweak contributions based on its order, that is

$$\alpha_\mu^{\mathrm{EW}} = \alpha_\mu^{\mathrm{EW}(1)} + \alpha_{\mu,\,b}^{\mathrm{EW}(2)} + \alpha_{\mu,\,f}^{\mathrm{EW}(2)} + \mathcal{O}(\alpha^{(3)}), \tag{4.4}$$

where the bracketed numbers indicate the order in perturbation, the subscripts b and f represent bosonic and fermionic contributions respectively, as represented in Figure 2. The higher, three-loop order as indicated by $\mathcal{O}(\alpha^{(0)}$, although dependent on the parametrisation used, is nonetheless heavily suppressed, of the order $\sim 0.4 \times 10^{-11}$ [14]. As such, its contribution to α_μ^{EW} is negligible.

The first order contribution can be expressed as

$$\alpha_\mu^{\mathrm{EW}(1)} = \frac{G_F}{\sqrt{8}} \frac{m_\mu^2}{8\pi^2} \left(\frac{5}{3} + \frac{1}{3}(1 - s_W^2) \right) + \mathcal{O}\left(\frac{m_\mu^2}{M_H^2} \right) + \mathcal{O}\left(\frac{m_\mu^2}{M_W^2} \right), \tag{4.5}$$

where G_F is the Fermi constant and $s_W^2 = 1 - (M_W/M_Z)^2$ is the weak mixing angle squared and m_μ, M_W, M_Z, M_H are the muon, W, Z and Higgs boson mass respectively. The first term in Equation 4.5 is the dominant factor since the second and third is heavily suppressed by the gauge bosons' mass squared, this gives us the first electroweak contribution of [14]

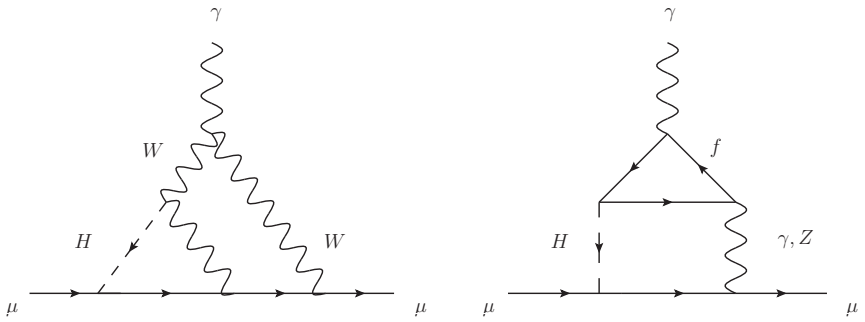

Figure 2: Feynman diagrams depicting second order electroweak contributions to the muon anomalous magnetic moment. **Left**: Higgs-dependent bosonic interaction. **Right**: triangular loop fermionic interaction.

$$\alpha_\mu^{\mathrm{EW}(1)} = (194.80 \pm 0.01) \times 10^{-11}, \tag{4.6}$$

where the uncertainty is due input parameters, namely, the mass of the W boson.

Since the determination of the Higgs boson mass, M_H in 2012, we can now compute the second order contributions. The bosonic part gives

$$\alpha_{\mu,\,b}^{\mathrm{EW}(2)} = (-19.97 \pm 0.03) \times 10^{-11}, \tag{4.7}$$

where the uncertainty is due to the determination of the Higgs mass. To that end, Gnendiger *et al.* have chosen to use the average central value from CMS and ATLAS experiments, giving $M_H = (125.6 \pm 1.5)\mathrm{GeV}$.

On the other hand, the right diagram in Figure 2 receives contributions from lepton and quark loops. It is to no surprise that this value has uncertainties dominated by quark interactions. Here, we give the value of $\alpha_\mu^{\mathrm{EW}(2)}$, determined from e, μ, u, c, d, s interactions

$$\alpha_\mu^{\mathrm{EW}(2)} = (-6.91 \pm 0.20 \pm 0.30) \times 10^{-11}, \tag{4.8}$$

where the first and second uncertainties are due to first and second generation quark interactions respectively. Neglecting the strongly suppressed three-loop contribution of order $\mathcal{O}(10^{-12})$ [2], this gives us a total of

$$\alpha_\mu^{\mathrm{EW}} = (153.6 \pm 1.0) \times 10^{-11}, \tag{4.9}$$

where the uncertainty is due to hadronic (quark and gluon) loop as seen in Figure 2 [2].

4.3 Hadronic Contributions - Preamble

Difficulties arise when we evaluate a_μ^{had} in the low energy regime. This is because the running strong coupling constant, α_s, becomes large around $E \lesssim 2\text{GeV}$ [1] and we are forced to abandon our perturbative methods used in evaluating the QED and electroweak contributions. Instead, we will explore the role of lattice QCD in calculating a_μ^{had}.

First, we will briefly illustrate the idea of computing quantum field theoretic observables on the lattice. To that end, we will follow the setup from Gattringer and Lang [16]. This amounts to a simple principle of discretising spacetime. We can do so by replacing continuous space by a finite 3D lattice, Λ_3. Given a smooth variable, $\vec{x} \in \mathbb{R}^3$, we have

$$\vec{x} \to a\vec{n}, \quad \text{with}\, \vec{n} = \begin{pmatrix} n_1 \\ n_2 \\ n_3 \end{pmatrix}, \tag{4.10}$$

where a is a constant known as the lattice spacing and $n_i \in \mathbb{Z}$ for $i = 1, 2, 3$. We see that $\vec{n}$ is now a lattice vector that moves us from one lattice site to another.

Similarly, fields which are originally functions of continuous spatial variable are now functions of coordinate vector of discrete spacing. For an arbitrary field operator, $\phi(\vec{x})$, we promote it to $\phi(\vec{x}) \to \phi(\vec{n})$. The generalisation to 4D spacetime is thus straightforward.

The lattice is to be implemented as an environment for numerical simulations. Thus, computing resources become one of the limiting factors. Since the lattice cannot span to infinity, we must impose boundary conditions. A suitable candidate would be periodic boundaries:

$$n_j = N \to n_j = 0, \tag{4.11}$$

for $j = 1, 2, 3$. This means that for a lattice of length $N \cdot a$, where $N \in \mathbb{Z}$, we consider the coordinate $n_j = N$ to be equivalent to the origin.

We need to transfer our knowledge of calculus onto the lattice as well. To that end, for a derivative such as $\nabla\phi$, we can approximate it as

$$\partial_j \phi(\vec{x}) \approx \frac{\phi(\vec{x} + \vec{j}) - \phi(\vec{x} - \vec{j})}{2a} + \mathcal{O}(a^2), \tag{4.12}$$

where $\vec{j}$ is another lattice vector that characterises the deviation from $\vec{n}$. The additional factor of $1/2$ in Equation 4.12 is to account for averaging the deviation from $\vec{n}$. Similarly, for an integral over space, we can discretise it as such

$$\int d^3x \to a^3 \sum_{\vec{n} \in \Lambda_3}, \tag{4.13}$$

which makes sense since we are now summing over the values associated to each discrete lattice site. It is easy to confirm the validity of these discretisations as we can always retrieve the contiuum expressions by taking the limit of $a \to 0$

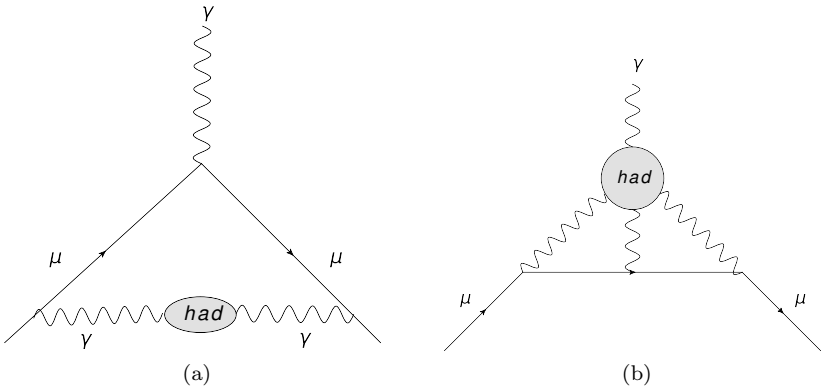

Figure 3: Feynman diagrams depicting hadronic contributions to the muon anomalous magnetic moment. **Left**: hadronic vacuum polarisation. **Right**: hadronic light-by-light scattering.

in Equation 4.12 and 4.13. For further details regarding the lattice formalism, we refer to the textbook by Gattringer and Lang [16].

In the following, we will explore how the implementation of the lattice can aide us in computing a_μ^{SM}. As stated in [1], the main theoretical uncertainty of a_μ is dominated by hadronic contributions. Namely, they come from two sources: the hadronic vacuum polarisation, a_μ^{HVP}, which comes in as second order electromagnetic corrections, and light-by-light scattering processes, a_μ^{HLbL}, which is present at third order. These are shown in Figure 3. For the most up-to-date progress on calculating the hadronic vacuum polarisation contributions, we will be following the review written by Della Morte *et al.* [17] in 2017. As for hadronic light-by-light processes, we will follow the progress made by Blum *et al.* [18] in 2016. We will also follow the conventions set up in [19]: the Minkowski signature is $(+\,-\,-\,-)$; Euclidean momenta are denoted by upper case Latin letters (K, Q etc.) and Minkowski momenta by lower case Latin letters (k, q etc.).

At the end of the following two subsections, we will compare the lattice approaches with alternative methods that are currently being studied.

4.4 Hadronic Vacuum Polarisation Contributions

Lattice calculations of a_μ^{HVP} are done by evaluating a convolution integral over the Euclidean momenta Q^2. This integral (to be defined below) receives the largest contribution when $Q^2 \approx m_\mu^2 \approx 0.01\mathrm{GeV}^2$, which corresponds to

$$
\begin{aligned}
Q &= \frac{2\pi}{L}, \\
L &= 2\pi Q^{-1}, \\
&\approx 2\pi 10^{-1}\text{GeV}^{-1}0.2\text{GeV fm}, \\
\Rightarrow L &\approx \mathcal{O}(10\text{fm}),
\end{aligned}
\tag{4.14}
$$

where L is the typical lattice length [17].

This becomes an issue as this low momentum falls below the smallest Fourier momentum in the typical lattice size. In particular, the problem lies in the ability to determine the vacuum polarisation function, $\Pi(Q^2)$, and the additive renormalisation term, $\Pi(0)$, accurately [17]. The paper by Dellta Morte [17] proposes two solutions:

1. Evaluate a_μ^{HVP} in time-momentum representation,
2. or represent the subtracted vacuum polarisation, $\Pi(Q^2) - \Pi(0)$, with Padé approximants using time-moments,

both of which we will discuss in detail below.

We will begin by collecting the tools necessary for lattice QCD. First, we need the electromagnetic current. Recall the piece of the electroweak Lagrangian concerning the quark sector,

$$
\mathcal{L} = i\bar{Q}_L\gamma^\mu D_\mu Q_L + i\bar{u}_R\gamma^\mu D_\mu u_R + i\bar{d}_R\gamma^\mu D_\mu d_R, \tag{4.15}
$$

where we have used the following convention [8],

$$
\begin{aligned}
Q_L^i &= \left(\begin{pmatrix} u \\ d \end{pmatrix}_L, \quad \begin{pmatrix} c \\ s \end{pmatrix}_L, \quad \begin{pmatrix} t \\ b \end{pmatrix}_L\right), \\
u_R^i &= (u_R, c_R, t_R), \\
d_R^i &= (d_R, s_R, b_R),
\end{aligned}
\tag{4.16}
$$

to indicate that the left-handed quarks transform as a doublet and the right-handed quarks transform as a singlet under SU(2)_L. The covariant derivative, D_μ, contains gauge fields which can be rearranged to give charged, neutral and electromagnetic interaction terms. The piece of the Lagrangian of interest to us is

$$
\begin{aligned}
\mathcal{L} &= ieA_\mu(C_1 i\bar{Q}_L\gamma^\mu Q_L + iC_2\bar{u}_R\gamma^\mu u_R + iC_3\bar{d}_R\gamma^\mu d_R), \\
C_1 &\equiv \begin{pmatrix} Y_u + T^3 & 0 \\ 0 & Y_d + T^3 \end{pmatrix}, \quad \text{where}\, T^3 = \frac{1}{2}\sigma^3, \\
C_{2,3} &= Y_{2,3},
\end{aligned}
\tag{4.17}
$$

where C_i are the charge matrices, Y_i is the hypercharge associated to the quarks and σ_3 is the third Pauli matrix. We note the absence of T^3 in C_2 and C_3 is due to the fact that they transform as a singlet under $\mathrm{SU(2)_L}$. Expanding the Lagrangian in Equation 4.15, and inserting the appropriate hypercharges to give the correct quark charges, we find that it simplifies to

$$\mathcal{L} = -eA_\mu \left(\frac{2}{3}\bar{u}\gamma^\mu u - \frac{1}{3}\bar{d}\gamma^\mu d - \frac{1}{3}\bar{s}\gamma^\mu s + ... \right), \tag{4.18}$$

where, for a given quark, $q = q_L + q_R$ and the ellipses denote the remaining heavier quarks. Using the fact that the above Lagrangian as a $\mathrm{U(1)_Y}$ symmetry, the electromagnetic current can be easily computed using Noether's theorem to give

$$J^\mu_{\mathrm{EM}} = \frac{2}{3}\bar{u}\gamma^\mu u - \frac{1}{3}\bar{d}\gamma^\mu d - \frac{1}{3}\bar{s}\gamma^\mu s + ... \tag{4.19}$$

With the electromagnetic current, J^μ_{EM}, we can construct the vacuum polarisation tensor in Euclidean space, which is defined as

$$\Pi_{\mu\nu}(Q) = \int d^4x\, e^{iQx} \langle J_\mu(x) J_\nu(0) \rangle, \tag{4.20}$$

where Q is the (Euclidean) momentum.

It turns out that gauge invariance provides a strong constraint on the form $\Pi_{\mu\nu}(Q)$ can take. From the Ward-Takahashi identity [6], we find that

$$Q_\mu \Pi^{\mu\nu}(Q) = 0, \tag{4.21}$$

where as usual, the repeated Lorentz indices are contracted. Together with Lorentz invariance, the most general tensor structure for $\Pi_{\mu\nu}$ is

$$\Pi_{\mu\nu}(Q) = \left(Q_\mu Q_\nu - \delta_{\mu\nu} Q^2 \right) \Pi(Q^2), \tag{4.22}$$

where $\delta_{\mu\nu}$ is the Euclidean metric and $\Pi(Q^2)$ is the vacuum polarisation function.

With the quantities defined above, we are now in the position to calculate the hadronic vacuum polrisation contribution to a_μ, which is defined as

$$a_\mu^{\mathrm{HVP}} = 4\alpha^2 \int_0^\infty dQ^2\, K(Q^2; m_\mu^2) \left(\Pi(Q^2) - \Pi(0) \right), \tag{4.23}$$

where α is the electromagnetic coupling constant and $K(Q^2; m_\mu^2)$ is a kernel function. The kernel here plays the role of an integral transform, intended to map the original domain (Euclidean momenta squared) to a different domain, where the evaluation of the integral may be easier.

In Equation 4.23, we find that the integral makes a significant contribution when $Q^2 \approx m_\mu^2 \approx 0.01\mathrm{GeV}^2$. As mentioned in the beginning paragrahs, the corresponding long wavelength regime is hard to evaluate on the lattice with available resources. Below, we will look at the solutions proposed by Della Morte [17].

4.4.1 Time Momentum Representation

Previously we introduced a kernel function, $K(Q^2; m_\mu^2)$, into Equation 4.23. It is precisely the mapping property of the kernel that we can exploit to circumvent the long wavelength problem. In this subsection, we will begin with the review on vector correlators by Bernecker *et al.* [19]. First, a slight change of notation: in literature it is often convenient to express the subtracted vacuum polarisation function as

$$\hat{\Pi}(Q^2) = 4\pi^2(\Pi(Q^2) - \Pi(0)), \tag{4.24}$$

where the $4\pi^2$ is present due to convention used. So Equation 4.23 is now

$$a_\mu^{\text{HVP}} = \left(\frac{\alpha}{\pi}\right)^2 \int_0^\infty dQ^2\, K(Q^2; m_\mu^2)\, \hat{\Pi}(Q^2). \tag{4.25}$$

In the time momentum representation, the subtracted vacuum polarisation, $\hat{\Pi}(Q^2)$, is proportional to the vector correlator, $G(x_0)$. This is a quantity that spatially sums the electromagnetic currents and it is defined as

$$G(t) = \int d^3x\, \langle J_z(t, \vec{x}) J_z^\dagger(0) \rangle, \tag{4.26}$$

where in Euclidean space, the spatial current is antiHermitian, $j_z^\dagger = -j_z$ [19]. We recognise that this is equivalent to the inverse Fourier transform of the vacuum polarisation tensor. In particular, the z-z component,

$$\begin{aligned} \Pi_{zz}(Q) &= \int d^4x\, \langle j_z(x) j_z(0) \rangle e^{i\omega t}, \\ &= \int dt\, d^3x\, \langle j_z(x) j_z(0) \rangle e^{i\omega t}, \\ &= \int dt\, G(t) e^{i\omega t}, \\ \Rightarrow G(t) &= \int \frac{d\omega}{2\pi} \Pi_{zz}(\omega, k^i = 0) e^{-i\omega t} \end{aligned} \tag{4.27}$$

The tensor structure of Π_{zz} follows from Equation 4.22,

$$\begin{aligned} \Pi_{zz}(Q) &= \left(Q_z Q_z - \delta_{zz} Q^2\right) \Pi(Q^2), \\ \Pi_{zz}(\omega, k^i = 0) &= \left(0 - \omega^2 - 0\right) \Pi(\omega, k^i = 0), \\ \Pi_{zz}(\omega) &= -\omega^2 \Pi(\omega). \end{aligned} \tag{4.28}$$

From Equation 4.27, we see that

$$\begin{aligned}
\Pi_{zz}(\omega, k^i = 0) &= \int dt\, G(t) e^{i\omega t}, \\
-\omega^2 \Pi(\omega^2) &= \int dt\, G(t) e^{i\omega t}, \\
\Pi(\omega^2) &= -\frac{1}{\omega^2} \int dt\, G(t) e^{i\omega t}.
\end{aligned} \tag{4.29}$$

We are interested in the infrared regime, where conventional lattice calculations face difficulties. Expanding the exponential as a power series, we have

$$\begin{aligned}
\Pi(\omega^2) &= \frac{-1}{\omega^2} \int dt\, G(t) \sum_{n=0}^{\infty} \frac{(i\omega t)^n}{n!}, \\
&= \frac{-1}{\omega^2} \int dt\, G(t) \left(1 + i\omega t + \frac{1}{2!}(i\omega t)^2 + \mathcal{O}(\omega^2)\right), \\
&= \frac{-1}{\omega^2} \left(\int dt\, G(t) + i\omega \int dt\, G(t) t - \frac{1}{2!}\omega^2 \int dt\, G(t) t^2 + \mathcal{O}(\omega^2)\right).
\end{aligned} \tag{4.30}$$

We note that the first integral on the final line vanishes as we can identify it as the quark number susceptibility of the vacuum. For the term linear in t, we note that $G(t)$ is an even function, so the integral of $G(t)$ with t - an odd function - across the boundaries therefore also vanishes. Keeping the first term, the subtracted vacuum polarisation function is thus

$$\begin{aligned}
\Pi(\omega^2) - \Pi(0) &= \int_{-\infty}^{\infty} dt\, G(t) \left(\frac{e^{-i\omega t} - 1}{\omega^2} + \frac{t^2}{2}\right), \\
&= \int_{-\infty}^{\infty} dt\, G(t) \left(\frac{\cos\omega t - 1}{\omega^2} + \frac{t^2}{2}\right), \\
&= \frac{2}{\omega^2} \int_0^{\infty} dt\, G(t) \left(\frac{\omega^2 t^2}{2} - (\cos\omega t - 1)\right), \\
\Pi(\omega^2) - \Pi(0) &= \frac{1}{\omega^2} \int_0^{\infty} dt\, G(t) \left(\omega^2 t^2 - 4\sin^2\frac{1}{2}\omega t\right),
\end{aligned} \tag{4.31}$$

where in going to the second line, we applied Euler's formula and noted that the $i \sin\omega t$ term is an odd function and causes the integral to vanish; in the following line, we gain a factor of 2 from the symmetric integration boundaries and this is used in the trigonometric identity to get the sine squared term in the final line. Inserting a factor of $4\pi^2$, we arrive at the desired modified expression

$$\hat{\Pi}(\omega^2) = 4\pi^2 \int_0^{\infty} dt\, G(t) \left(t^2 - \frac{4}{\omega^2} \sin^2 \frac{1}{2}\omega t\right). \tag{4.32}$$

Now, we may rewrite our expression for $a_\mu^{\rm HVP}$,

$$\begin{aligned} a_\mu^{\rm HVP} &= \left(\frac{\alpha}{\pi}\right)^2 \int_0^\infty dQ^2\, K(Q^2; m_\mu^2)\, \hat{\Pi}(Q^2), \\ &= \left(\frac{\alpha}{\pi}\right)^2 4\pi^2 \int_0^\infty \frac{d\omega^2}{\omega^2}\, dt\, K(\omega^2; m_\mu^2)\, G(t) \left(\omega^2 t^2 - 4\, \sin^2\, \frac{1}{2}\omega t\right), \end{aligned} \tag{4.33}$$

$$\begin{aligned} a_\mu^{\rm HVP} &= \left(\frac{\alpha}{\pi}\right)^2 \int_0^\infty dt\, \tilde{K}(t; m_\mu)\, G(t), \\ \text{with} \quad \tilde{K}(t; m_\mu) \equiv \tilde{f}(t) &= 4\pi^2 \int_0^\infty \frac{d\omega^2}{\omega^2}\, K(\omega^2; m_\mu^2)\, \left(\omega^2 t^2 - 4\, \sin^2\, \frac{1}{2}\omega t\right), \end{aligned} \tag{4.34}$$

where $\tilde{K}(t; m_\mu)$ is the time-momentum representation of the original kernel.

In order to evaluate $a_\mu^{\rm HVP}$, we need the correct expression for $\tilde{K}(t; m_\mu)$. For the remainder of this subsection, we will refer to [17] to derive the appropriate expression that can be used on the lattice. Further, we will use $\tilde{K}(t; m_\mu)$ and $\tilde{f}(t)$ interchangeably and similarly for $K(\omega^2; m_\mu^2)$ and $f(\omega^2)$.

First, we can simplify $\tilde{K}(t; m_\mu)$ a little more,

$$\begin{aligned} d\omega^2 &= \omega\, d\omega, \\ \Rightarrow \tilde{K}(t; m_\mu) &= 8\pi^2 \int_0^\infty \frac{d\omega}{\omega}\, K(\omega^2; m_\mu^2)\, \left(\omega^2 t^2 - 4\, \sin^2\, \frac{1}{2}\omega t\right). \end{aligned} \tag{4.35}$$

Since $a_\mu^{\rm HVP}$ is a dimensionless unit, we can deduce that the mass dimensions of $\tilde{f}(t)$ is -2 since the integral measure dt has mass dimensions -1 and the $G(t)$ term has 4 copies of Dirac fermions integrated over 3-space, giving mass dimensions $\frac{3}{2}\cdot 4 - 3 = 3$. Therefore, $m_\mu^2 \tilde{f}(t)$ would make a dimensionless function of $m_\mu t$. For the moment, we will set m_μ to unity. Once we obtain an expression for $\tilde{f}(t)$ we will restore the appropriate factors by dimensional analysis.

The function $f(\omega^2)$, which is really $K(\omega^2; m_\mu^2)$ in disguise, has the following form

$$f(\omega^2) = \frac{1}{\omega\sqrt{\omega^2+4}} - 1 + \frac{\omega}{2}(\sqrt{\omega^2+4} - \omega), \tag{4.36}$$

for $\omega > 0$. We introduce an auxillary function, $\tilde{g}_\epsilon(t)$ as

$$\tilde{g}_\epsilon(t) = \int_0^\infty \frac{d\omega}{\sqrt{\omega^2+\epsilon^2}} f(\omega^2+\epsilon^2)\, \cos\omega t, \tag{4.37}$$

where we have introduced an infrared regulator, ϵ, to keep $\tilde{g}_\epsilon(t)$ from diverging in the long wavelength limit where $\omega \to 0$. Using the auxillary function, we can identity the following

$$
\begin{aligned}
\int_0^\infty \frac{d\omega}{\omega} f(\omega^2) &= \lim_{\epsilon\to 0} \tilde{g}_\epsilon(0), \\
\int_0^\infty \frac{d\omega}{\omega} f(\omega^2)\omega^2 t^2 &= \lim_{\epsilon\to 0}(-1)\cdot \frac{\mathrm{d}^2\tilde{g}_\epsilon(t)}{\mathrm{d}t^2}\bigg|_{t=0}\cdot t^2, \\
&= \lim_{\epsilon\to 0} -\tilde{g}''_\epsilon(0)t^2, \\
\int_0^\infty \frac{d\omega}{\omega} f(\omega^2)\, 4\sin^2\frac{1}{2}\omega t &= \int_0^\infty \frac{d\omega}{\omega} f(\omega^2)\, 2(1-\cos\omega t), \\
&= \lim_{\epsilon\to 0}\, 2(\tilde{g}_\epsilon(0) - \tilde{g}_\epsilon(t)).
\end{aligned}
\tag{4.38}
$$

Collecting all the terms together, we can re-express $\tilde{f}(t)$ as

$$
\begin{aligned}
8\pi^2\int_0^\infty \frac{d\omega}{\omega}\, f(\omega^2)(\omega^2 t^2 - 4\sin^2\frac{1}{2}\omega t) &= 8\pi^2 \lim_{\epsilon\to 0} -\tilde{g}''_\epsilon(0)t^2 - 2(\tilde{g}_\epsilon(0) - \tilde{g}_\epsilon(t)), \\
\tilde{f}(t) &= 16\pi^2 \lim_{\epsilon\to 0} \tilde{g}_\epsilon(t) - \tilde{g}_\epsilon(0) - \frac{1}{2}\tilde{g}''_\epsilon(0)t^2.
\end{aligned}
\tag{4.39}
$$

Consider the $\tilde{g}_\epsilon(t)$ piece. When expanded out, it reads

$$
\begin{aligned}
\tilde{g}_\epsilon(t) &= \int_0^\infty \frac{d\omega}{\sqrt{\omega^2+\epsilon^2}} \left(\frac{1}{\sqrt{\omega^2+\epsilon^2}\sqrt{\omega^2+\epsilon^2+4}} - 1 \right. \\
&\qquad \left. + \frac{\sqrt{\omega^2+\epsilon^2}}{2}(\sqrt{\omega^2+\epsilon^2+4} - \sqrt{\omega^2+\epsilon^2}) \right) \cos\omega t, \\
&= \int_0^\infty d\omega\, \frac{\cos\omega t}{(\omega^2+\epsilon^2)\sqrt{\omega^2+4}} - \frac{\cos\omega t}{\sqrt{\omega^2+\epsilon^2}} \\
&\qquad + (\sqrt{\omega^2+4} - \sqrt{\omega^2+\epsilon^2})\,\frac{\cos\omega t}{2},
\end{aligned}
\tag{4.40}
$$

where in going to the second line, we remove some infrared regulators as they are no longer needed to make the integral convergent. Let's focus on the first term in the integrand, that is

$$
I(t) = \int_0^\infty d\omega\, \frac{\cos\omega t}{(\omega^2+\epsilon^2)\sqrt{\omega^2+4}}. \tag{4.41}
$$

This integral is difficult to evaluate from brute force integration. Instead, we turn $I(t)$ into a differential equation that satisfies the following initial conditions

$$
\begin{aligned}
I''(t) - \epsilon^2 I(t) &= -K_0(2t), \\
I(0) = \frac{\pi}{4\epsilon} - \frac{1}{4} + \mathcal{O}(\epsilon) \qquad & I'(0) = 0,
\end{aligned}
\tag{4.42}
$$

where $K_0(2t)$ is the modified Bessel function of the second kind [20] and the primes indicate time derivatives as usual. For the inhomogenous case, we can express $K_0(2t)$ with an integral representation [20],

$$K_0(t) = \int_1^\infty du\, \frac{e^{-ut}}{\sqrt{u^2-1}}. \tag{4.43}$$

Rescaling $K_0(t)$ with $t \to 2t$ and $u \to \frac{1}{2}u$, we find

$$K_0(2t) = \int_2^\infty du\, \frac{e^{-ut}}{\sqrt{u^2-4}}. \tag{4.44}$$

Now we focus on the left hand side of the differential equation. For the particular solution, we can take the Laplace transform of $I_p(t)$ [21],

$$I_p(t) = \int_0^\infty du\, e^{-ut}\tilde{I}(u), \tag{4.45}$$

and match $\tilde{I}(u)$ with the right hand side. Doing so, we find that

$$I_p''(t) - \epsilon^2 I_p(t) = (u^2-\epsilon^2)\int_0^\infty du\, e^{-ut}\tilde{I}(u). \tag{4.46}$$

If we look up a table of integral transforms, for example see [21], we find that the explicit expression for $\tilde{I}(u)$ is

$$\tilde{I}(u) = -\frac{H(u-2)}{(u^2-\epsilon^2)\sqrt{u^2-4}}, \tag{4.47}$$

where $H(u-2)$ is the Heaviside step function. The particular solution is thus

$$I_p(t) = \int_2^\infty du\, \frac{e^{-ut}}{u^2\sqrt{u^2-4}}, \tag{4.48}$$

where we allow $\epsilon \to 0$ as Equation 4.48 is a valid solution to the differential equation. We note that $I_p(0) = -\frac{1}{4}$ and $I'(0) = \frac{\pi}{4}$. Combining the particular solution with a general solution, $I_0(t)$, and taking into account the initial conditions, we find the exact expression

$$
\begin{aligned}
I_\epsilon(t) &= I_0(t) + I_p(t), \\
\text{using } I_\epsilon(0) &= \frac{\pi}{4\epsilon} - \frac{1}{4} + \mathcal{O}(\epsilon), \\
\frac{\pi}{4\epsilon} - \frac{1}{4}_{\mathcal{O}}(\epsilon) &= I_0(0) - \frac{1}{4}, \\
\Rightarrow I_0(0) &= \frac{\pi}{4\epsilon}, \\
\text{using } I'_\epsilon(0) &= 0, \\
0 &= I'(0) + \frac{\pi}{4}, \\
I'(0) &= -\frac{\pi}{4}, \\
I(t) = -\frac{\pi}{4}t + C, & \\
\text{since } I(0) &= \frac{\pi}{4\epsilon} + \mathcal{O}(\epsilon), \\
\Rightarrow C &= \frac{\pi}{4\epsilon} + \mathcal{O}(\epsilon),
\end{aligned}
\tag{4.49}
$$

$$
\therefore \qquad I_\epsilon(t) = \frac{\pi}{4}(\frac{1}{\epsilon} - t) + I_p(t) + \mathcal{O}(\epsilon). \tag{4.50}
$$

Now, consider the second integrand in Equation 4.40, that is

$$
\int_0^\infty d\omega \, \frac{\cos \omega t}{\sqrt{\omega^2 + \epsilon^2}}. \tag{4.51}
$$

For later use, we note one of the useful forms of the n'th modified Bessel function of the second kind [20],

$$
K_n(t) = \frac{\Gamma(n + \frac{1}{2})(2t)^n}{\sqrt{\pi}} \int_0^\infty d\omega \, \frac{\cos \omega}{(t^2 + \omega^2)^{n+\frac{1}{2}}}, \tag{4.52}
$$

where $\Gamma(n + \frac{1}{2})$ is the gamma function. In particular, for half-integer argument, we apply the reflection relation [22]:

$$
\Gamma(n)\Gamma(1 - n) = \frac{\pi}{\sin n\pi}. \tag{4.53}
$$

Comparing Equation 4.51 with 4.52, we identify that $K_0(t)$ is needed. Under the rescaling $\omega \to \omega\epsilon$, Equation 4.51 matches with $K_0(\epsilon t)$ as

$$
\begin{aligned}
\int_0^\infty \epsilon d\omega \, \frac{\cos \epsilon\omega t}{\sqrt{\epsilon^2\omega^2 + \epsilon^2}} &= \int_0^\infty d\omega \, \frac{\cos \epsilon\omega t}{\sqrt{\omega^2 + 1}}, \\
&= K_0(\epsilon t),
\end{aligned}
\tag{4.54}
$$

after $K_0(\epsilon t)$ undergoes $\omega \to \omega t$ to restore the correct argument in the cosine and to simultaneously remove the t^2 factor in the denominator.

We obtain the third term in a similar fashion. Note that this integral will be convergent in the long wavelength limit, where $\omega \to 0$, so to make the computation easier we can set the infrared regulator, ϵ, to zero:

$$\int_0^\infty \frac{d\omega}{2} \left(\sqrt{\omega^2+4} - \omega\right) \cos\,\omega t \tag{4.55}$$

We begin by identifying we need the $n = 1$ version of Equation 4.52:

$$\begin{aligned} K_1(2t) &= \frac{\Gamma(\frac{3}{2})4t}{\sqrt{\pi}} \int_0^\infty d\omega\, \frac{\cos\omega}{(4t^2+\omega^2)^{\frac{3}{2}}}, \\ &\text{rescaling } \omega \to \omega t, \\ K_1(2t) &= \frac{2}{t} \int_0^\infty d\omega\, \frac{\cos\omega t}{(\omega^2+4)^{\frac{3}{2}}}, \end{aligned} \tag{4.56}$$

where we have used the fact that $\Gamma(\frac{3}{2}) = \frac{\sqrt{\pi}}{2}$. To match Equation 4.55 with 4.56, we need to integrate by parts twice,

$$\begin{aligned} \int_0^\infty \frac{d\omega}{2} \left(\sqrt{\omega^2+4} - \omega\right) \cos\omega t &= \frac{1}{2t} \sin\omega t \left(\sqrt{\omega^2+2} - \omega\right)\Big|_0^\infty \\ &\quad - \frac{1}{2t} \int_0^\infty d\omega\, \sin\omega t \left(\frac{\omega}{\sqrt{\omega^2+4}} - 1\right), \\ &= \frac{1}{2t} \left(\frac{\omega}{\sqrt{\omega^2+4}} - 1\right) \cos\omega t\Big|_0^\infty \\ &\quad - \frac{1}{2t^2} \int_0^\infty d\omega \left(\frac{1}{\sqrt{\omega^2+4}} - \frac{\omega^2}{(\omega^2+4)^{\frac{3}{2}}}\right) \cos\omega t, \\ &= \frac{1}{2t^2} \left(1 - \frac{4t}{t} \int_0^\infty d\omega\, \frac{\cos\omega t}{(\omega^2+4)^{\frac{3}{2}}}\right), \end{aligned} \tag{4.57}$$

where in the first line, the integrated term vanish at both limits and in the second line, the integrated term vanishes as $\omega \to \infty$ but leaves a factor of $1/2t^2$ at $\omega = 0$. Thus, we can write Equation 4.55 in terms of $K_1(2t)$:

$$\int_0^\infty \frac{d\omega}{2} \left(\sqrt{\omega^2+4} - \omega\right) \cos\,\omega t = \frac{1}{2t^2}(1 - 2tK_1(2t)\,). \tag{4.58}$$

Finally, we can combine all three results to rewrite $\tilde{g}_\epsilon(t)$:

$$\tilde{g}_\epsilon(t) = \frac{\pi}{8\epsilon}(e^{ut} + e^{-ut}) + I_p(t) - K_0(\epsilon t) + \frac{1}{2t^2}(1 - 2tK_1(2t)\,) + \mathcal{O}(\epsilon). \tag{4.59}$$

With this explicit version of $\tilde{g}_\epsilon(t)$, we can subtitude this back into Equation 4.39. Let's consider it term by term, starting with the first on the r.h.s:

$$
\begin{aligned}
16\pi^2 \lim_{\epsilon\to 0} \tilde{g}_\epsilon(t) &= 16\pi^2 \lim_{\epsilon\to 0} \left(\frac{\pi}{4}(\frac{1}{\epsilon} - t) + I_p(t) - K_0(\epsilon t) + \frac{1}{2t^2}(1 - 2tK_1(2t)) + \mathcal{O}(\epsilon) \right), \\
&= 2\pi^2 \left(\lim_{\epsilon\to 0} \left(\frac{\pi}{4\epsilon} - K_0(\epsilon t) \right) + 2\pi t + 8I_p(t) + \frac{4}{t^2} - \frac{8}{t} K_1(2t) \right).
\end{aligned} \tag{4.60}
$$

With foresight, we claim that the $\frac{\pi}{4\epsilon}$ term will cancel with another copy in the $\tilde{g}_\epsilon(0)$ term. For now, we focus on the $K_0(\epsilon t)$ term. First, we note that the modified Bessel functions of the second kind can be expressed as sum formulas [20]. For the n'th order, we have

$$
\begin{aligned}
K_n(t) = \frac{1}{2}\left(\frac{1}{2}t\right)^{-n} \sum_{k=0}^{n-1} \frac{(n-k-1)!}{k!}(-\frac{1}{4}t^2)^k + (-1)^{n+1}\log(\frac{1}{2}t)\, I_n(t) \\
+ (-1)^n \frac{1}{2}\left(\frac{1}{2}t\right)^n \sum_{k=0}^{\infty} \left(\psi(k+1) + \psi(n+k+1)\right) \frac{(\frac{1}{4}t^2)^k}{k!(n+k)!},
\end{aligned} \tag{4.61}
$$

where $I_n(t)$ is the modified Bessel function of the first kind [23] and $\psi(z)$ is the digamma function [24], which has the following crucial property:

$$
\psi(1) = -\gamma, \tag{4.62}
$$

where γ is the Euler-Mascheroni constant [25]. In particular, for $n = 0$ we have

$$
\begin{aligned}
K_0(\epsilon t) &= -\log(\frac{1}{2}\epsilon t)\, I_0(\epsilon t) + \sum_{k=0}^{\infty} \psi(k+1) \frac{(\frac{1}{4}\epsilon t^2)^k}{k!(n+k)!}, \\
&= -\log(\frac{1}{2}\epsilon t)\, I_0(\epsilon t) + \psi(1) + \mathcal{O}(\epsilon^2 t^2), \\
K_0(\epsilon t) &= -\log(\frac{1}{2}\epsilon)\, I_0(\epsilon t) - \log(t) I_0(\epsilon t) - \gamma + \mathcal{O}(\epsilon^2 t^2),
\end{aligned} \tag{4.63}
$$

where we group the ϵ terms of quadratic order and above as they will tend to zero when we take the limit. Once again, with foresight, we leave the first term on the r.h.s as it will cancel with a similar term in the $\tilde{g}_\epsilon(0)$ term. Plugging this back into Equation 4.60, we find

$$
\begin{aligned}
16\pi^2 \lim_{\epsilon\to 0} \tilde{g}_\epsilon(t) = 16\pi^2 \left(\lim_{\epsilon\to 0} \left(\frac{\pi}{4\epsilon} + \log(\frac{1}{2}\epsilon)\, I_0(\epsilon t) \right) - \frac{\pi}{4}t + I_p(t) \right. \\
\left. + \frac{1}{2t^2} - \frac{8}{t} K_1(2t) + \log(t) + \gamma \right),
\end{aligned} \tag{4.64}
$$

where we note that in the limit of $\epsilon \to 0$, $I_0(\epsilon t) \to 1$.

Now, we can focus on the second term in Equation 4.39,

$$\lim_{\epsilon\to 0}\tilde{g}_\epsilon(0) = \lim_{\epsilon\to 0}\left[\frac{\pi}{4}\left(\frac{1}{\epsilon}-t\right) + I_p(t) - K_0(\epsilon t) \right. \\ \left. \frac{1}{2t^2}\left(1-2tK_1(2t)+\mathcal{O}(\epsilon)\right)\right]\Bigg|_{t=0},$$

$$\lim_{\epsilon\to 0}\tilde{g}_\epsilon(0) = \lim_{\epsilon\to 0}\left(\frac{\pi}{4\epsilon} - K_0(\epsilon t) + \frac{1}{2t^2}(1-2tK_1(2t))\right)\Bigg|_{t=0} - \frac{1}{4}, \tag{4.65}$$

where, as promised, the $\frac{\pi}{4\epsilon}$ term in Equation 4.65 will cancel with that in Equation 4.60. The $K_0(\epsilon t)$ term proceeds as above and cancels the factor of γ in Equation 4.64. Consider the second term of Equation 4.65: for $n = 1$,

$$\begin{aligned} K_1(2t) &= \frac{1}{2t} + \log(t)\, I_1(2t) - \frac{t}{2}\left(\psi(1)+\psi(2)+\mathcal{O}(t^2)\right), \\ &\text{where } \psi(1)+\psi(2) = 1-2\gamma, \\ \Rightarrow \frac{1}{2t^2}(1-2tK_1(2t)) &= \frac{1}{2t^2} - \left(\frac{1}{2t^2} + \frac{1}{t}\log(t)\, I_1(2t) - \frac{1}{2}(1-2\gamma+\mathcal{O}(t^2))\right), \\ &= -\frac{1}{t}\log(t)\, I_1(2t) + \frac{1}{2} - \gamma - \mathcal{O}(t^2). \end{aligned} \tag{4.66}$$

So, in Equation 4.65, we now have

$$\begin{aligned} \lim_{\epsilon\to 0}\tilde{g}_\epsilon(0) = \lim_{\epsilon\to 0}\Bigg(&\frac{\pi}{4\epsilon} + \log(\frac{1}{2}\epsilon)\, I_0(\epsilon t) + \log(t) I_0(\epsilon t) + \gamma \\ &-\frac{1}{t}\log(t)\, I_1(2t) + \mathcal{O}(\epsilon^2 t^2)\Bigg)\Bigg|_{t=0} - \gamma + \frac{1}{2} - \frac{1}{4}, \\ \Rightarrow \lim_{\epsilon\to 0}\tilde{g}_\epsilon(0) = \lim_{\epsilon\to 0}\Bigg(&\frac{\pi}{4\epsilon} + \log(\frac{1}{2}\epsilon)\, I_0(\epsilon t) + \log(t) I_0(\epsilon t) + \gamma \\ &-\frac{1}{t}\log(t)\, I_1(2t) + \mathcal{O}(\epsilon^2 t^2)\Bigg)\Bigg|_{t=0} - \gamma + \frac{1}{4}. \end{aligned} \tag{4.67}$$

Now we can focus on the final term on the r.h.s of Equation 4.39. It involves taking the derivatives of $\tilde{g}_\epsilon(t)$:

$$
\begin{aligned}
\tilde{g}_\epsilon''(t) &= \frac{d^2}{dt^2}\left(\frac{\pi}{4}\left(\frac{1}{\epsilon}-t\right)+I_p(t)-K_0(\epsilon t)+\frac{1}{2t^2}(1-2tK_1(2t)\right), \\
&= \frac{d}{dt}\left(-\frac{\pi}{4}+I_p'(t)-\epsilon\frac{dK_0(\epsilon t)}{d(\epsilon t)}-\frac{1}{t^3}-\frac{2}{t}\frac{dK_1(2t)}{d(2t)}+\frac{1}{t^2}K_1(2t)\right), \\
&= \left(I_p''(t)-\epsilon^2\frac{d^2K_0(\epsilon t)}{d(\epsilon t)^2}+\frac{3}{t^4}+\frac{2}{t^2}\frac{dK_1(2t)}{d(2t)}-\frac{4}{t}\frac{d^2K_1(2t)}{d(2t)^2}\right. \\
&\qquad\qquad \left.-\frac{2}{t^3}K_1(2t)+\frac{4}{t^2}\frac{dK_1(2t)}{d(2t)}\right),
\end{aligned}
\tag{4.68}
$$

The key observation to tackling this term is that the derivative of the modified Bessel functions of the second kind have simple expressions. They are:[2]

$$
\begin{aligned}
\frac{d^2K_0(\epsilon t)}{d(\epsilon t)^2} &= \frac{1}{2}(K_0(\epsilon t)+K_2(\epsilon t)), \\
\frac{dK_1(2t)}{d(2t)} &= \frac{1}{2}(K_0(2t)+K_2(2t)), \\
\frac{d^2K_1(2t)}{d(2t)^2} &= \frac{1}{2}(3K_1(2t)+K_3(2t)).
\end{aligned}
\tag{4.69}
$$

For easier manipulations, we express them in series formula again. For notational brevity, let the above modified Bessel functions be functions of a general variable t, where we will restore the correct arguments afterwards, we have:

[2] citation needed; I worked it out on mathematica

$$
\begin{aligned}
K_0(t) + K_2(t) &= -\log\frac{1}{2}t\, I_0(t) + \sum_{k=1}^{\infty}\psi(k+1)\frac{(\frac{1}{4}t^2)^k}{(k!)^2} + \frac{2}{t^2}\sum_{k=0}^{1}\frac{(1-k)!}{k!}(-\frac{1}{4}t^2)^k \\
&\quad - \log\frac{1}{2}t\, I_2(t) - \overbrace{\frac{1}{8}t^2\sum_{k=0}^{\infty}(\psi(k+1)+\psi(k+2))\frac{(\frac{1}{4}kt^2)^k}{k!(k+2)!}}^{=0 \text{ due to } t^2 \text{ out front}}, \\
&= -(I_0(t)+I_2(t))\log\frac{1}{2}t + \gamma + \frac{2}{t^2} - \frac{1}{2}\mathcal{O}(t^2), \\
3K_1(t) + K_3(t) &= \frac{3}{t} + 3\log\frac{1}{2}t\, I_1(t) - \overbrace{\frac{3}{4}t\sum_{k=0}^{\infty}(\psi(k+1)+\psi(k+2))\frac{(\frac{1}{4}t^2)^k}{k!(k+1)!}}^{\text{vanishes when t=0}} \\
&\qquad + \frac{4}{t^3}\sum_{k=0}^{2}\frac{(2-k)!}{k!}(-\frac{1}{4}t^2)^k + \log\frac{1}{2}t\, I_3(t) \\
&\qquad - \overbrace{\frac{1}{16}t^3\sum_{k=0}^{\infty}(\psi(k+1)+\psi(k+4))\frac{(\frac{1}{4}t^2)^k}{k!(k+3)!}}^{=0 \text{ due to } t^3 \text{ out front}}, \\
&= \log\frac{1}{2}t\,(3I_1(t)+I_3(t)) + \frac{2}{t} + \frac{8}{t^3} + \frac{t}{8}
\end{aligned}
\tag{4.70}
$$

The term which we are interested in is $\frac{t}{8}$ in $3K_1(t) + K_3(t)$. With the correct arguments restored, it appears in Equation 4.68 as

$$
\begin{aligned}
\tilde{g}_\epsilon''(t) &= \cdots \frac{4}{t}\cdot\frac{1}{2}(3K_1(2t)+K_3(2t))\cdots, \\
&= \cdots + \frac{2}{t}(\frac{t}{8}) + \cdots, \\
\Rightarrow \frac{1}{2}\tilde{g}_\epsilon(0)t^2 &= \frac{t^2}{8},
\end{aligned}
\tag{4.71}
$$

where the ellipses denote the unimportant contributions from Equation 4.70.

At last, we can combine Equation 4.64, 4.67 and 4.71 to obtain an explicit expression of $\tilde{f}(t)$:

$$
\begin{aligned}
\tilde{f}(t) &= 16\pi^2 \lim_{\epsilon\to 0}\tilde{g}_\epsilon(t) - \tilde{g}_\epsilon(0) - \frac{1}{2}\tilde{g}_\epsilon''(0)t^2, \\
\tilde{f}(t) &= 16\pi^2(\log t - \frac{\pi}{4}t + I_p(t) + \frac{1}{2t^2} - \frac{1}{t}K_1(2t) - \gamma - \frac{1}{4} - \frac{t^2}{8}).
\end{aligned}
\tag{4.72}
$$

Recall that before we began deriving this expression, we set the muon mass to unity. We must take extra care now that we are restoring the units, since the

r.h.s contains t terms, which have mass dimensions -1. Since we claimed in the above that $\tilde{f}(t)$ has mass dimensions -2, an immediate corollary is that $m_\mu^2 \tilde{f}(t)$ would be a dimensionless function of variable $\hat{t} = m_\mu t$. Restoring the proper units, we finally have

$$\tilde{f}(t) = \frac{2\pi^2}{m_\mu^2}(8\log\hat{t} - 2\pi\hat{t} + 8I_p(\hat{t}) + \frac{4}{\hat{t}^2} - \frac{8}{\hat{t}}K_1(2\hat{t}) - 8\gamma - 2 - \hat{t}^2). \tag{4.73}$$

Thus, we now have an explicit expression for the kernel function, $\tilde{K}(t; m_\mu)$ from Equation 4.34. In principle, we can now calculate a_μ due to the hadronic vacuum polarisation, one contribution for each quark flavour. However, as noted in [17], due to the finite nature of the time direction on the lattice, the difficulty in this approach arises as the Euclidean correlator, $G(t)$, is integrated to infinite time. Della Morte *et al.* propose various solutions to this problem. It begins by first splitting the Euclidean correlator into two parts

$$G(t) = \begin{cases} G(t)_{\text{inter}}, & t \leq t^{\text{cut}} \\ G(t)_{\text{ext}}, & t > t^{\text{cut}} \end{cases}, \tag{4.74}$$

where t^{cut} is a free parameter, set based on a choice which balances statistical error and systematic effects on the final value of a_μ^{HVP}. $G(t)_{\text{inter}}$ can be obtained from interpolation of numerical data and $G(t)_{\text{ext}}$ from extrapolating the correlator using an infinite sum of exponentials. For more details regarding the specific choice of t^{cut} and computing $G(t)_{\text{ext}}$ in a finite volume, we refer to [17] and [19].

4.4.2 Time Moments and Padé Approximants

In §4.4.1, we derived an explicit expression for the kernel function such that we may evaluate a_μ^{HVP}. Here we explore another method, which involves calculating time moments such that they may be used to construct Padé representations for the subtracted vacuum polarisation function, $\hat{\Pi}(Q^2)$ [17].

First, we need to introduce an approximation which builds on our knowledge of Taylor expansions. Given a function, $f(x)$, that is analytic about the origin, we can write the Taylor expansion at $x = 0$ as

$$f(x) = \sum_{n=0}^{\infty} f^{(n)}(0)x^n, \quad \text{where } f^{(n)}(0) \equiv \frac{1}{n!}\frac{d^n f}{dx^n}\bigg|_{x=0}. \tag{4.75}$$

Next, suppose there exists an approximation of $f(x)$ called $P(x)$ and suppose it agrees with $f(x)$ up to some degree k [26]. We can express this as

$$f(x) - P(x) = \sum_{n=k+1}^{\infty} f^{(n)}(0)x^n = \mathcal{O}(x^{k+1}) \tag{4.76}$$

If $P(x)$ can be expressed as a rational function, that is, a ratio of polynomials, then $P(x)$ is a Padé approximant of order m/n [26], denoted as

$$P(x)[m/n] = \frac{\sum_{i=0}^{m} a_i x^i}{1 + \sum_{j=1}^{n} b_j x^j}, \tag{4.77}$$

where $m, n \in \mathbb{Z}$. If the original function $f(x)$ is known, then the coefficients, a_i and b_j can be determined with successive derivatives of $f(x)$ evaluated at the origin. Naturally, the Padé approximant with increasing order in m and n will yield increasingly better approximations of the original function.

Back to evaluating the hadronic vacuum polarisation contribution to a_μ, we recall that the exact shape of the vacuum polarisation function, $\Pi(Q^2)$, and its additive renormalisation, $\Pi(0)$, is difficult to determine to the demanded accuracy in the infrared regime, corresponding to $Q^2 \approx 0.01\text{GeV}^2$ [17]. As an alternate method to the time-momentum representation, Della Morte *et al.* [17] proposes that we replace the vacuum polarisation function, $\Pi(\omega^2)$ in Equation 4.34 with its Padé approximant. So, we write

$$\Pi(\omega^2)[m/n] = \frac{\sum_{i=0}^{m} a_i \omega^{2i}}{1 + \sum_{j=1}^{n} b_j \omega^{2j}}. \tag{4.78}$$

The next task is to determine the exact value of these expansion coefficients. To that end, Della Morte *et al.* proposes two methods that are currently used in research:

1. determine a_j and b_j from vacuum polarisation function fits obtained from simulations,
2. or subtituting time moments in place of the coefficients a_i and b_j.

In this section, we will explore the second option. As in §4.4.1, this will be based on the paper by Della Morte [17].

For convenience, we restate a couple of the results we had from the beginning paragraphs of §4.4. We recall the the quark polarisation tensor is the Fourier transform of the vector correlator,

$$\Pi_{\mu\nu}(Q) = \int d^4x \, e^{iQx} \langle J_\mu(x) J_\nu(0) \rangle. \tag{4.79}$$

Due to Lorentz and O(4) invariance [19], the tensor structure of $\Pi_{\mu\nu}(Q)$ has the form

$$\Pi_{\mu\nu}(Q) = \left(Q_\mu Q_\nu - \delta_{\mu\nu} Q^2\right) \Pi(Q^2). \tag{4.80}$$

For low Q^2, corresponding to the infrared regime, we can expand the vacuum polarisation function for $Q^2 = 0$,

$$\Pi(Q^2) = \Pi_0 + \sum_{n=1}^{\infty} \Pi_n Q^{2n}, \tag{4.81}$$

where $\Pi_0 \equiv \Pi(0)$ and Π_n is the n'th expansion coefficient. Choosing $Q = (\omega, 0)$ as before, we find that

$$\omega^2\Pi(\omega^2) = \int_{-\infty}^{\infty} dt\, e^{i\omega t} G(t) \tag{4.82}$$

and the vacuum polarisation function is now modified as

$$\Pi(\omega^2) = \Pi_0 + \sum_{n=1}^{\infty} \Pi_n \omega^{2n}, \tag{4.83}$$

We now define the time moment as

$$G_{2n} = \int_{-\infty}^{\infty} dt\, t^{2n} G(t). \tag{4.84}$$

In light of the quantities we prepared prior to the definition, we establish the following relation,

$$\begin{aligned} G_{2n} &= \int_{-\infty}^{\infty} dt\, t^{2n} G(t), \\ &= \int_{-\infty}^{\infty} dt\, (i)^{2n} \frac{\partial^{2n}}{\partial \omega^{2n}} e^{i\omega t}\Big|_{\omega=0} G(t), \\ &= (-1)^n \frac{\partial^{2n}}{\partial \omega^{2n}} \int_{-\infty}^{\infty} dt\, e^{i\omega t} G(t)\Big|_{\omega=0}, \\ G_{2n} &= (-1)^n \frac{\partial^{2n}}{\partial \omega^{2n}} \omega^2 \Pi(\omega^2)\Big|_{\omega=0}, \end{aligned} \tag{4.85}$$

Together with Equation 4.83, we can express the time moments in terms of the vacuum polarisation function at low ω^2:

$$\begin{aligned} G_{2n} &= (-1)^n \frac{\partial^{2n}}{\partial \omega^{2n}} \omega^2 \Pi(\omega^2)\Big|_{\omega=0}, \\ G_{2n} &= (-1)^n \frac{\partial^{2n}}{\partial \omega^{2n}} (\omega^2 \Pi_0 + \sum_{m=1}^{\infty} \Pi_m \omega^{2m+2})\Big|_{\omega=0}, \end{aligned} \tag{4.86}$$

Let us compute the first few orders of n,

$$\begin{aligned} &\text{for } n = 1, \\ &\quad G_2 = -\frac{\partial^2}{\partial \omega^2} (\omega^2 \Pi_0 + \sum_{m=1}^{\infty} \Pi_m \omega^{2m+2})\Big|_{\omega=0}, \\ &\qquad = -(2\Pi_0 + \sum_{m=1}^{\infty} (2m+2)(2m+1)\Pi_m \omega^{2m})\Big|_{\omega=0}, \\ &\Rightarrow \Pi_0 = -\frac{1}{2} G_2, \end{aligned} \tag{4.87}$$

$$
\begin{aligned}
&\text{for } n = 2, \\
&\quad G_4 = (-1)^2 \frac{\partial^4}{\partial \omega^4} (\omega^2 \Pi_0 + \sum_{m=1}^{\infty} \Pi_m \omega^{2m+2}) \Big|_{\omega=0}, \\
&\quad\quad = \frac{\partial^4}{\partial \omega^4} (\Pi_1 \omega^4 + \Pi_2 \omega^6 + \mathcal{O}(\omega^8)) \Big|_{\omega=0}, \\
&\quad\quad = 4! \Pi_1 + 6 \cdot 5 \cdot 4 \cdot 3 \Pi_2 \omega^2 + \mathcal{O}(\omega^4)) \Big|_{\omega=0}, \\
&\quad \Rightarrow \Pi_1 = \frac{1}{4!} G_4,
\end{aligned}
\tag{4.88}
$$

and similarly for $n = 3$, we have

$$
\begin{aligned}
&\text{for } n = 3, \\
&\quad G_4 = (-1)^3 \frac{\partial^6}{\partial \omega^6} (\Pi_1 \omega^4 + \Pi_2 \omega^6 + \mathcal{O}(\omega^8)) \Big|_{\omega=0}, \\
&\quad\quad = -6! \Pi_2 + \mathcal{O}(\omega^2)) \Big|_{\omega=0}, \\
&\quad \Rightarrow \Pi_2 = -\frac{1}{6!} G_6
\end{aligned}
\tag{4.89}
$$

Thus, we establish a relation between the vacuum polarisation function and the time moments,

$$
\Pi(\omega^2) = -\frac{1}{2} G_2 + \sum_{n=1} \frac{G_{2n+2}}{(2n+2)!} (-1)^{n+1} \omega^{2n}, \tag{4.90}
$$

where $n = 1, 2, 3....$ Note that in Equation 4.87, we have established a relation between the additive renormalisation and a known quantity: G_2. Thus, determining the additive renormalisation $\Pi(0)$ using time moments amounts to summing the vector correlator over all Euclidean time.

It is precisely these time moments, G_{2n+2} and their relation to the expansion coefficients of $\Pi(\omega^2)$ as $\omega = 0$ that allows us to construct a Padé approximant for the vacuum polarisation function. Using the parametrisation proposed in [27], we can rewrite the Padé approximant in a more useful form

$$
P(\omega^2)[m/n] = \omega^2 \left(a_0 \, \delta_{m,n+1} + \sum_{k=1}^{n} \frac{a_k}{b_k + \omega^2} \right) \tag{4.91}
$$

By comparing each derivative of the Padé approximant with the corresponding derivative of the vacuum polarisation function evaluated at $\omega^2 = 0$, we can determine the expansion coefficients of the Padé approximant in terms of Π_i, with $i = 1, 2, 3..., n$. For example, let us consider the Padé approximant of order $m = n = 1$. Let $x = \omega^2$, we have

$$
\begin{aligned}
P(x)[1/1] &= \frac{a_1 x}{b_1 + x}, \\
P'(0)[1/1] &= \left(\frac{a_1}{b_1 + x} - \frac{a_1 x}{(b_1 + x)^2} \right) \Bigg|_{x=0}, \\
&= \frac{a_1}{b_1}, \\
\Rightarrow \Pi_1 &= \frac{a_1}{b_1}, \\
P''(0)[1/1] &= \left(-\frac{2a_1}{(b_1 + x)^2} + \frac{a_1 x}{(b_1 + x)^{3/2}} \right) \Bigg|_{x=0}, \\
&= -\frac{2a_1}{b_1^2}, \\
\text{since } \Pi''(0) &= 2\Pi_2, \\
\Rightarrow a_1 &= -b_1^2 \, \Pi_2, \\
\Rightarrow b_1 = -\frac{\Pi_1}{\Pi_2} \quad &\text{and} \quad a_1 = -\frac{\Pi_1^2}{\Pi_2}
\end{aligned}
\tag{4.92}
$$

Putting the expresisons for a_1 and b_1 back into Equation 4.91, we find

$$
\begin{aligned}
P(x)[1/1] &= x \frac{-\frac{\Pi_1^2}{\Pi_2}}{-\frac{\Pi_1}{\Pi_2} + x}, \\
&= \frac{x\Pi_1^2}{\Pi_1 - x\Pi_2}, \\
\Rightarrow P(\omega^2)[1/1] &= \frac{\omega^2 \Pi_1^2}{\Pi_1 - \omega^2 \Pi_2},
\end{aligned}
\tag{4.93}
$$

Now, with Equation 4.90, we can subtitute the corresponding time moments in place of Π_i to obtain a Padé approximant of order 1,1 for the vacuum polarisation function, $\Pi(\omega^2)$. Just as in §4.4.1, evaluating the time moments involves integrating the correlators over all Euclidean times. To perform this on the lattice, strategies to circumvent the problem of infinite time proposed in [17] can be employed.

For completeness, we note that lattice calculations of a_μ^{HVP} can be compared with a semi-phenomenological approach. Guided by the requirement of causality [1] and by the optical theorem [28], we can relate the vacuum polarisation amplitude to the total cross section in e^+e^- annihilation processes as such:

$$
\begin{aligned}
\Pi(k^2) - \Pi(0) &= \frac{k^2}{\pi} \int_0^\infty fs \, \frac{\mathrm{Im}\,\Pi(s)}{s(s - k^2 - i\epsilon}, \\
\text{with} \quad \mathrm{Im}\,\Pi(s) &\equiv \frac{s}{4\pi\alpha(s)} \sigma_{\mathrm{tot}}(e^+e^- \to \text{hadrons})
\end{aligned}
\tag{4.94}
$$

where s is the centre-of-mass energy squared and we have specialised the cross section to have hadronic final states. Using experimental data for the cross section, this method produces $a_\mu^{\rm HVP} = 6923(42)(3) \times 10^{-11}$, where the first error is due to systematic uncertainties and the second is due to perturbative QCD at intermediate and large energy regime [2].

On the other hand, when we use the two lattice approaches derived above, we independently get [17]

$$\begin{aligned} a_\mu^{\rm HVP,TMR} &= (616.7 \pm 24.8 \pm 28.9) \times 10^{-10}, \\ a_\mu^{\rm HVP,hybrid} &= (623.1 \pm 25.4 \pm 19.7) \times 10^{-10}{}^{3}, \end{aligned} \tag{4.95}$$

where the first uncertainty is due to statistical error and the second is due to systematic error.

4.5 Hadronic Light-by-Light Contribution

In this section, we look at the second hadronic contribution to $a_\mu^{\rm had}$. This is due to a process known as the hadronic light-by-light scattering and it is illustrated in Figure 3 and 4 below. In contrast to the vacuum polarisation contributions, there are no known methods to determine hadronic light-by-light (henceforth abbreviated as HLbL) scattering processes from experimental data or dispersion relation [18]. Thus, they are not as well studied. A starting point, as suggested by the title of this review, is to calculate the HLbL contributions from first principles by means of lattice QCD. We will be predominantly following the paper written by Blum *et al.* [18] in this section to review possible options for computing HLbL processes on the lattice.

It is clear from Figure 4 that these contributions begin at the $\mathcal{O}(\alpha^3)$ order. They involve a fermion loop with four photons attached to it [1]. In our case, we specialise the case to a $q-\bar{q}$ loop. The identical nature of the photons means there are $3! = 6$ different configurations for the internal photons (labelled by Lorentz indices σ, κ, ρ), so one would expect six amplitudes contributing to $a_\mu^{\rm HLbL}$ at $\mathcal{O}(\alpha^3)$ order.

In order to express $a_\mu^{\rm HLbL}$ in terms that can be computed on the lattice, we begin from the field theoretic point of view and tailor it to yield quantites that can be evaluated using lattice QCD. Following [6], we start with the Dirac equation for a fermion field, ψ,

$$(i\not{\partial} - m)\psi = 0, \tag{4.96}$$

where $\not{\partial} \equiv \gamma^\mu \partial_\mu$ and γ^μ are the four gamma matrices. The contraction of Lorentz indices, μ is also assumed. In momentum space, we can decompose ψ into different modes,

[3] The superscript 'hybrid' stands for the use of time moments as coefficients for the Padé approximants.

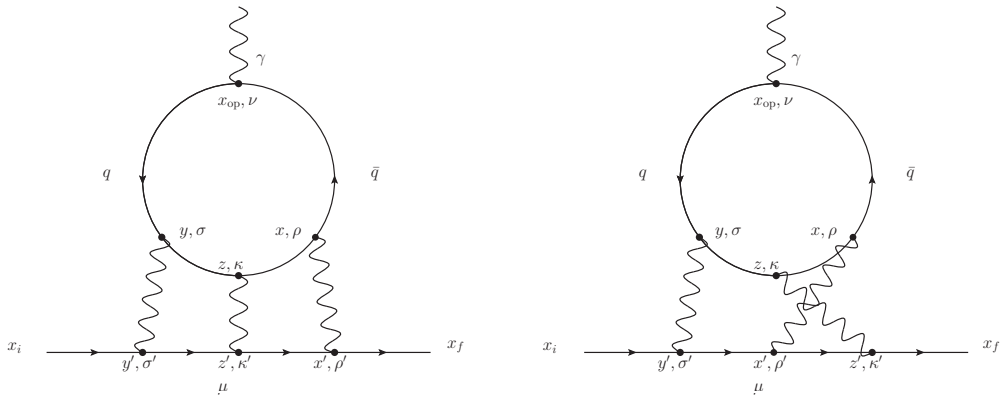

Figure 4: Feynman diagrams depicting hadronic light-by-light contributions to the muon anomalous magnetic moment. Above are two of the 6 possible contributions, each a unique permutation of the internal photon propagator with the external muon line.

$$\psi(x) = \int \frac{d^4p}{(2\pi)^4}\, u(p) e^{ip\cdot x}, \tag{4.97}$$

where $u(p)$ are the plane wave solutions [29]. In momentum space, Equation 4.96 then becomes

$$(\not{p} - m)u(p) = 0. \tag{4.98}$$

If we multiply on the left hand side of Equation 4.98 with a factor of $\bar{u}(p)\gamma^\mu$ and add to it the complex conjugate, we obtain the Gordon decomposition:

$$\begin{aligned}
\bar{u}(p')(\gamma^\mu(\not{p} - m) + (\not{p}' - m)\gamma^\mu)u(p) &= 0, \\
\bar{u}(p')(\gamma^\mu \not{p} + \not{p}'\gamma^\mu - 2m\gamma^\mu)u(p) &= 0, \\
\frac{1}{2m}\bar{u}(p')(\gamma^\mu\gamma^\nu p_\nu + \gamma^\nu p'_\nu \gamma^\mu)u(p) &= \bar{u}(p')\gamma^\mu u(p), \\
\frac{1}{2m}\bar{u}(p')((\eta^{\mu\nu} - iS^{\mu\nu})p_\nu + (\eta^{\mu\nu} + iS^{\mu\nu})p'_\nu)u(p) &= \bar{u}(p')\gamma^\mu u(p), \\
\bar{u}(p')\left(\frac{\eta^{\mu\nu}(p_\nu + p'_\nu)}{2m} + \frac{iS^{\mu\nu}(p'_\nu - p_\nu)}{2m}\right)u(p) &= \bar{u}(p')\gamma^\mu u(p), \\
\bar{u}(p')\left(\frac{(p+p')^\mu}{2m} + \frac{iS^{\mu\nu}(p'_\nu - p_\nu)}{2m}\right)u(p) &= \bar{u}(p')\gamma^\mu u(p),
\end{aligned} \tag{4.99}$$

where $S^{\mu\nu} = \frac{1}{2}[\gamma^\mu, \gamma^\nu]$. With foresight [6], we note that the second term on the l.h.s involves the spin of the fermion due to the presence of the gamma matrices, and it is this term that gives the magnetic moment.

Next, we consider the matrix element of the electromagnetic current. Sandwiched between the muon initial and final state of momentum and spin p, s and p', s' respectively, Lorentz invariance and current conservation gives us

$$\langle p', s'|J^{\mu}(0)|p, s\rangle = -e\bar{u}(p', s')\left(\gamma^{\mu}F_1(q^2) + \frac{iS^{\mu\nu}q_{\nu}}{2m}F_2(q^2)\right)u(p, s). \quad (4.100)$$

where $q = p' - p$ is the momentum transfer and $F_i(q^2)$ with $i = 1, 2$ are called form factors. Now, we can apply the Gordon decomposition derived in Equation 4.99 and obtain

$$\begin{aligned}\langle p', s'|J^{\mu}(0)|p, s\rangle = -e\bar{u}(p', s')\left(\left(\frac{(p+p')^{\mu}}{2m} + \frac{iS^{\mu\nu}q_{\nu}}{2m}\right)F_1(q^2)\right. \\ \left. + \frac{iS^{\mu\nu}q_{\nu}}{2m}F_2(q^2)\right)u(p, s).\end{aligned} \quad (4.101)$$

For small q^2, we can expand the form factors. Considering only terms up to linear order in q,

$$\begin{aligned}\langle p', s'|J^{\mu}(0)|p, s\rangle = -e\bar{u}(p', s')\left(\left(\frac{(p+p')^{\mu}}{2m} + \frac{iS^{\mu\nu}q_{\nu}}{2m}\right)(F_1(0)\right. \\ \left. + q^2F_1'(0) + \mathcal{O}(q^4)) + \frac{iS^{\mu\nu}q_{\nu}}{2m}(F_2(0) + q^2F_2'(0) + \mathcal{O}(q^4))\right)u(p, s).\end{aligned} \quad (4.102)$$

$$\langle p', s'|J^{\mu}(0)|p, s\rangle = -e\bar{u}(p', s')\left(\frac{(p+p')^{\mu}}{2m}F_1(0) + \frac{iS^{\mu\nu}q_{\nu}}{2m}(F_1(0) + F_2(0))\right)u(p, s). \quad (4.103)$$

We can identify the first term in the brackets on the r.h.s as the electric charge [6] of the muon, which can be experimentally observed. The interesting piece contains the magnetic moment of the muon, quantified as $F_1(0) + F_2(0)$. Since $F_1(0)$, by definition, is set to unity, any shifts in the leptonic magnetic moment, for example, due to HLbL scattering processes, will be captured by $F_2(0)$. Thus, we find that [18]

$$a_{\mu} = F_2(0). \quad (4.104)$$

On the lattice, we work with the l.h.s of Equation 4.103. This establishes a method of comparison between theoretical (l.h.s) and experimentally measured (r.h.s) values. This involves evaluating Euclidean space Green's functions, which contains a muon source and sink with definite incoming and outgoing momenta. According to Blum *et al.* [18], this is chosen as $\vec{Q}/2$ and $-\vec{Q}/2$ respectively, where we remain notationally consistent with $\vec{Q}$ denoting the Euclidean momentum.

In Euclidean space, the l.h.s of Equation 4.103 becomes

$$\langle \mu(x_f) J^{\nu}(x_{\rm op}) \bar{\mu}(x_i) \rangle, \tag{4.105}$$

which is to be interpreted as a muon being created at the source, denoted by $\vec{x}_i$, where it interacts with the photon and is annihilated at the sink, denoted by $\vec{x}_f$. This quantity is equal to the product of electric charge and the amplitude of the process, $-e\mathcal{M}(\vec{x}_i, \vec{x}_{\rm op}, \vec{x}_f)$, which is defined as

$$\mathcal{M}_{\nu}(\vec{Q}) = \lim_{\substack{t_i \to -\infty \\ t_f \to \infty}} e^{E(t_f - t_i)} \sum_{\vec{x}_i, \vec{x}_f} e^{-i\frac{\vec{Q}}{2}(\vec{x_i} + \vec{x_f})} e^{i\vec{Q}\cdot\vec{x}_{op}} \mathcal{M}_{\nu}(x_i, x_{\rm op}, x_f). \tag{4.106}$$

where $E = \sqrt{m_{\mu}^2 + |\vec{Q}/2|^2}$. We now have an equation for computing the total amplitude of an electromagnetic interaction on the lattice. In Equation 4.106, we sum over all local amplitudes $\mathcal{M}_{\nu}(x_i, x_{\rm op}, x_f)$ due to every possible sink-source combination on the lattice volume. We note that the exponential factor $e^{-i\vec{Q}/2(\vec{x}_f - \vec{x}_i)}$ was included to ensure that the total amplitude on the l.h.s is translation invariant.

As mentioned in the opening paragraph of this section, there are $3! = 6$ different Feynman diagrams to consider, each corresponding to different arrangement of the internal photons as illustrated in Figure 4. We can thus re-express the amplitude $\mathcal{M}_{\nu}(x_i, x_{\rm op}, x_f)$ as the sum of these six graphs' amplitude. This can be done by summing over the Feynman amplitudes with different spacetime configurations as

$$\mathcal{M}_{\nu}(x_i, x_{\rm op}, x_f) = \sum_{x,y,z} \mathcal{F}_{\nu}(x, y, z, x_{\rm op}, x_i, x_f), \tag{4.107}$$

where x, y, z are spacetime points as seen in Figure 4. These specific Feynman amplitudes can be deduced from Feynman rules, easily compiled in texts such as [29]. Schematically, we have

$$\begin{aligned} \mathcal{F}_{\nu}(x, y, z, x_{\rm op}, x_i, x_f) \equiv \quad & \text{“all possible internal quark lines”} \\ & \times \text{“internal photon propagators”} \\ & \times \text{“permutations of internal muon propogators”}. \end{aligned} \tag{4.108}$$

Formally, it is written as

$$\begin{aligned} \mathcal{F}_{\nu}(x, y, z, x_{\rm op}, x_i, x_f) &= -(-ie)^3 \\ &\times \sum_{q \in \{u,d,s\}} (ie_q)^4 \, \langle \, \mathrm{Tr}[\gamma_{\nu} S_q(x_{\rm op}, x) \gamma_{\rho} S_q(x, z) \gamma_{\kappa} S_q(z, y) \gamma_{\sigma} S_q(y, x_{\rm op})]_{\rm QCD} \rangle \\ &\times \sum_{x', y', z'} G_{\rho\rho'}(x, x') G_{\kappa\kappa'}(z, z') G_{\sigma\sigma'}(y, y') \\ &\times \left(S_{\mu}(x_f, x') \gamma_{\rho'} S_{\mu}(x', z') \gamma_{\kappa'} S_{\mu}(z', y') \gamma_{\sigma'} S_{\mu}(y', x_i) + 5 \text{ other permutations} \right), \end{aligned} \tag{4.109}$$

where S_μ are the muon propagators, $G_{\alpha\alpha'}$ with $\alpha \in \{\rho, \kappa, \sigma\}$ are the photon propagators and S_q are the internal quark propagators. The cubic factor of $-ie$ at the front comes from the coupling between the internal photon propagator with the muon line. The QCD subscript of the trace represents an average over all QCD gauge configutations. This is responsible for providing the background fields in which the quark propagators can be computed on. The $-e$ and e_q are the muon and quark electric charge respectively, where $e_q = 2e/3$ or $-e/3$ depending on the quark in context.

During the time of writing this paper [18] in 2015, it is computationally expensive to evaluate $\mathcal{F}_\nu$ directly on the lattice. Below, we explore two stochastic methods proposed by Blum *et al.* to circumvent the problem of computing resources.

4.5.1 Exact Photon Propogators

To introduce random sampling using Equation 4.109 directly is computationaly expensive, even with a single QCD configuration. To that end, we express the total amplitude $\mathcal{M}_\nu(\vec{Q})$ as an explicit sum of three additional spacetime vertices, x, y, z at which the internal photon line couples to the quark line

$$\mathcal{M}_\nu(\vec{Q}) = e^{i\vec{Q}\cdot\vec{x}_{\text{op}}} \sum_{x,y,z} \mathcal{F}_\nu(\vec{Q}, x, y, z, x_{\text{op}}), \tag{4.110}$$

where we note that the Feynman amplitude now depends on the Euclidean momentum, $\vec{Q}$, as well. As before, the factor of $e^{i\vec{Q}\cdot\vec{x}_{\text{op}}}$ is present to maintain translation invariance of $\mathcal{M}_\nu(\vec{Q})$. It is also independent of the time of propogation, t_{op}. We can identify this modified Feynman amplitude as

$$\mathcal{F}_\nu(\vec{Q}, x, y, z, x_{\text{op}}) = \lim_{\substack{t_i \to -\infty \\ t_f \to \infty}} e^{E(t_f - t_i)} \sum_{\vec{x}_i, \vec{x}_f} e^{-i\frac{\vec{Q}}{2}(\vec{x_i} + \vec{x_f})} \mathcal{F}_\nu(x, y, z, x_i, x_{\text{op}}, x_f) \tag{4.111}$$

from Equation 4.106. Blum *et al.* then make an arbitrary choice and let $\vec{Q} = \frac{2\pi}{L}\vec{z}$, where L is the spatial extent of the lattice. Since the muons are fermions, their propogators, S_μ are evaluated in the z-direction with anti-periodic boundary conditions, that is,

$$\psi(P) = -\psi(0), \tag{4.112}$$

where P denotes the period. This is to ensure that trace of an operator remains consistent in the path integral formalism for fermions [30].

We will now exploit the spacetime translation covariance of $F_\nu(\vec{Q}, x, y, z, x_{\text{op}})$. Starting with Equation 4.110, we rewrite the arguments that describe the spacetime positions relative to the quark loop. This involves shifting the position variables of F_ν by the average, $w = \frac{x+y}{2}$. In Equation 4.110, this translates to

$$\begin{aligned}\mathcal{M}_\nu(\vec{Q}) &= \sum_{x,y,z} e^{i\vec{Q}(\vec{x}_{\rm op}-\vec{w})}\mathcal{F}_\nu(\vec{Q}, x-w, y-w, z-w, x_{\rm op}-w),\\ &= \sum_{x,y,z} e^{i\vec{Q}(\vec{x}_{\rm op}-\vec{w})}\mathcal{F}_\nu(\vec{Q}, \frac{x-y}{2}, -\frac{x-y}{2}, z-w, x_{\rm op}-w),\\ &= \sum_r \left(\sum_{\tilde{z},\tilde{x}_{\rm op}} e^{i\vec{Q}\cdot\tilde{\vec{x}}_{\rm op}}\mathcal{F}_\nu(\vec{Q}, \frac{r}{2}, -\frac{r}{2}, \tilde{z}, \tilde{x}_{\rm op}) \right),\end{aligned} \tag{4.113}$$

where we have introduced a notational shorthnd for the shifted variables, $\tilde{z} = z-w$ and $\tilde{x}_{\rm op} = x_{\rm op}-w$. In going from the second line to the third, we note that summing over x and y after the shift by the average is equivalent to summing over the $r = x-y$ values, so we can replace the two spacetime summations with r, which is performed only after we have completely summed over the shifted z-direction and the propogation coordinates.

Equation 4.113 gives a natural strategy to evaluate on the lattice. First, we make a random choice to w somewhere within the spacetime volume. To ensure that $t_f - t_i$ is large in accordance to Equation 4.106, corresponding to the limit $t \to \pm\infty$, we choose, in context of the lattice

$$\begin{aligned} t_i &= (x_{\rm op})_0 - \frac{T}{4},\\ t_f &= (x_{\rm op})_0 + \frac{T}{4},\end{aligned} \tag{4.114}$$

where T is the temporal extent of the lattice volume. The coordinate r can be used to introduce stochastic effects. We can employ $r/2$ and $-r/2$ as source locations of two propogators whose sinks are joined at the shifted positions $\tilde{z}$ and $\tilde{x}_{\rm op}$. When summed over w and r and averaged over the QCD gauge configurations, Equation 4.113 gives the muon-current 3-point function.

This method has an advantage that in the limit of infinite volume on the lattice, we only have finite statistical noise.

4.5.2 Obtaining $q^2 = 0$ in Finite Volume

In this method, we work with the matrix element of the electromagnetic current in Equation 4.101. For convenience, we restate it here:

$$\begin{aligned}\langle p', s'|J^\mu(0)|p, s\rangle = \bar{u}(p', s') \Bigg(\left(\frac{(p+p')^\mu}{2m} + \frac{iS^{\mu\nu}q_\nu}{2m} \right) F_1(q^2)\\ + \frac{iS^{\mu\nu}q_\nu}{2m} F_2(q^2) \Bigg) u(p, s).\end{aligned} \tag{4.115}$$

This contains the form factor $F_2(q^2)$ multiplied with components of momentum transfer q_ρ. Speacialising in Euclidean momentum, $F_2(Q^2)$ can be obtained

from lattice calculation when $Q_\rho \neq 0$ such that $a_\mu = F_2(0)$ can be determined in the limit of $Q_\rho \to 0$. However, this is difficult to perform on the lattice since the smallest non-zero momentum component is $\frac{2\pi}{L}$, where L is the spatial extent of the lattice. Thus, in the limit of $Q_\rho \to 0$ we require $L \to \infty$, which corresponds to the infinite volume limit. A solution to the problem of finite computation resource is to define a spatial moment for the Feynman amplitude, which in turn determines the matrix element of $J_\nu(0)$, as we will see below.

We begin with Equation 4.113. For convenience, we drop the tilde on the shifted variables

$$\mathcal{M}_\nu(\vec{Q}) = \sum_r \left(\sum_{z,x_{\text{op}}} e^{i\vec{Q}\cdot\vec{x}_{\text{op}}} \mathcal{F}^c_\nu(\vec{Q}, \frac{r}{2}, -\frac{r}{2}, z, x_{\text{op}}) \right), \tag{4.116}$$

where we have also added a superscript c in foresight of working towards the electromagnetic current. $\mathcal{F}^c_\nu$ has the same dependence on x_{op} as J_ν, which means it also obeys the same Ward identity. This can be expressed as

$$\Delta_{(\text{op})\nu} F^c_\nu(\vec{Q}, x, y, z, x_{\text{op}}) = 0, \tag{4.117}$$

where the contraction of the Lorentz index ν is implied. We also remind ourselves that in Euclidean space, the covariant and contravariant indices bear no distinction. Here, $\Delta_{(\text{op})\nu}$ is the backwards lattice measure of change, defined as

$$\Delta_x f(x) = f(x) - f(x-a), \tag{4.118}$$

which we recall is the difference in values of f between neighbouring lattice sites, where a is the lattice spacing.

Now, the key step is to replace $e^{i\vec{Q}\cdot\vec{x}_{\text{op}}}$ with $e^{i\vec{Q}\cdot\vec{x}_{\text{op}}} - 1$, giving

$$\mathcal{M}_\nu(\vec{Q}) = \sum_r \left(\sum_{z,x_{\text{op}}} \mathcal{F}^c_\nu(\vec{Q}, \frac{r}{2}, -\frac{r}{2}, z, x_{\text{op}})(e^{i\vec{Q}\cdot\vec{x}_{\text{op}}} - 1) \right). \tag{4.119}$$

This is perfectly consistent with Equation 4.116 since the factor of -1 introduced will vanish due to the Ward identity. This is demonstrated below, with arguments suppressed,

$$\begin{aligned} \sum_{r,z,x_{\text{op}}} \Delta_\nu F_\nu &= 0, \\ \sum_{r,z,x_{\text{op}}} x\Delta_\nu F_\nu &= 0, \\ \Rightarrow \sum_{r,z,x_{\text{op}}} x_\rho \Delta_\nu F_\nu &= \sum_{r,z,x_{\text{op}}} \Delta_\nu(x_\rho F_\nu) - \sum_{r,z,x_{\text{op}}} \delta_{\rho\nu} F_\nu, \\ 0 &= -\sum_{r,z,x_{\text{op}}} F_\rho, \end{aligned} \tag{4.120}$$

which is as we claimed in the paragraph above, assuming that the surface term $\Delta_\nu(x_\rho F_\nu)$ goes to zero sufficiently fast upon summation.

Now, we can expand Equation 4.119 in $\vec{Q}$ from both the exponential and the amplitude. Once again, we suppress the irrelevant arguments to prevent a cluttering of notation. To linear order in small $\vec{Q}$,

$$\begin{aligned}\mathcal{M}_\nu(\vec{Q}) &= \sum_r \left(\sum_{z,x_{\rm op}} (\mathcal{F}^c_\nu(0) + Q_j \frac{\partial \mathcal{F}^c_\nu}{\partial Q_j}\Big|_{Q=0} + \mathcal{O}(Q^2))(1 + iQ_k \cdot x_{{\rm op},k} + \mathcal{O}(Q^2) - 1) \right), \\ &= \sum_r \left(\sum_{z,x_{\rm op}} (iQ_k \cdot x_{{\rm op},k} \mathcal{F}^c_\nu(0) + \mathcal{O}(Q^2) \right),\end{aligned} \tag{4.121}$$

taking the derivative of $\vec{\mathcal{Q}}$ and evaluating it at $\vec{Q} = 0$,

$$\begin{aligned}\frac{\partial}{\partial Q_j}\mathcal{M}_\nu(0) &= \sum_r \left(\sum_{z,x_{\rm op}} (i\delta_{jk} \cdot x_{{\rm op},k} \mathcal{F}^c_\nu(0) + \mathcal{O}(Q) \right) \Big|_{Q=0}, \\ &= i \sum_r \sum_{z,x_{\rm op}} \mathcal{F}^c_\nu(0)\, x_{{\rm op},j},\end{aligned} \tag{4.122}$$

This equation is derived in an infinite spacetime volume, captured by the fact that $\mathcal{M}_\nu(\vec{Q})$ has neither spacetime dependence nor arguments in $x_{\rm op}$. However, since $\mathcal{F}^c_\nu$ is a function of r and $-r$, the average, by symmetry, is location at the origin. which means that F^c_ν deceases exponenetially with increasing $|x_{\rm op}|$. In terms of lattice QCD, this implies that the summation can be carried out in a large but nonetheless finite volume with exponentially small corrections.

We want to make contact with the form factor, $F_2(0)$ in Equation 4.115 since this is where we can compute a_μ. We know that the l.h.s of Equation 4.115 is equal to $-e\mathcal{M}_\nu$. In Euclidean space,

$$-e\mathcal{M}_\nu(Q) = -e\bar{u}(Q',s') \left(\left(\frac{(Q+Q')^\mu}{2m} - \frac{iS^{\mu\nu}Q_\mu}{2m} \right) F_1(Q^2) - \frac{iS^{\mu\nu}Q_\mu}{2m} F_2(Q^2) \right) u(Q,s), \tag{4.123}$$

where we picked up a minus sign for the Q_μ terms due to the relabelling $\mu \to \nu$ and $\nu \to \mu$.

In the limit of $t_i \to -\infty$ and $t_f \to \infty$, $u(Q,s$ and $\bar{u}(Q',s')$ become energy eigenstates of the free theory Hamiltonian [29]. This allow us to write

$$u(Q) = \frac{-i\not{Q}^- + m_\mu}{2E} \quad \text{and} \quad \bar{u}(Q') = \frac{-i\not{Q}'^+ + m_\mu}{2E}, \tag{4.124}$$

where $Q^{\pm} = (iE, \pm\vec{Q}/2)$ and $E = \sqrt{m_\mu^2 + |\vec{Q}/2|^2}$. Equation 4.123 now takes the following form

$$\mathcal{M}_\nu(Q) = -\left(\frac{-i\not{Q}'^{+} + m_\mu}{2E}\right)\left(\frac{iS^{\mu\nu}Q_\mu}{2m}F_2(Q^2)\right)\left(\frac{-i\not{Q}^{-} + m_\mu}{2E}\right), \quad (4.125)$$

where we have omitted the $F_1(Q^2)$ term since we are only interested in contributions to a_μ.

To make contact with Equation 4.122, we expand the r.h.s of Equation 4.125 to linear order in the limit of small momentum transfer, $Q = 0$. Then, take the derivative with respect to Q_i and then evaluate the expression at $Q = 0$. For the moment, define $f^-(Q) = (-i\not{Q}^{-} + m_\mu)/2E$ and similarly for the primed positive energy solution as the expansion in the limit of small Q,

$$\begin{aligned}\frac{\partial}{\partial Q_i}\mathcal{M}_\nu(Q)\Big|_{Q=0} &\approx \frac{\partial}{\partial Q_i}\Bigg[-f'^{+}(Q)\left(\frac{iS^{\mu\nu}Q_\mu}{2m}(F_2(0)\right. \\ &\quad \left. + Q^2\frac{\partial^2}{\partial Q^2}F_2(Q^2)) + \mathcal{O}(Q^4)\right) f^-(Q)\Bigg]\Bigg|_{Q=0}, \\ &= -f'^{+}(Q)\left(\frac{iS^{\mu\nu}}{2m}\delta_{i\mu}F_2(0)\right) f^-(Q)\Big|_{Q=0} + \cdots,\end{aligned} \quad (4.126)$$

where the $\cdots$ denote terms including derivatives of f'^{+} and f^-, which will vanish when $Q = 0$ due to the Q_ν coupled to $F_2(Q^2)$. Now if we sandwich Equation 4.126 with zero momentum positive energy eigenstates, $\bar{u}(s')$ and $u(s)$, on the r.h.s we get the term

$$-\bar{u}(s)f'^{+}(Q)\left(\frac{iS^{i\nu}}{2m}F_2(0)\right) f^-(Q)\Big|_{Q=0} u(s) \quad (4.127)$$

Now, if we write out explicitly the expansions $f'^{+}(Q)$ and $f^-(Q)$, we have

$$
\begin{aligned}
\frac{1}{E} &= \frac{1}{\sqrt{m_\mu^2 + |\frac{Q}{2}|^2}}, \\
\frac{1}{E} &\approx \frac{1}{m_\mu} - \frac{1}{2!}\frac{Q^2}{m_\mu^3} + \mathcal{O}(Q^4), \\
\Rightarrow \frac{-iQ'^{+} + m_\mu}{2E} &= (-i(\gamma^0(iE) + \gamma^k Q_k) + m_\mu)\frac{1}{2}\left(\frac{1}{m_\mu} - \frac{1}{2!}\frac{Q^2}{m_\mu^3} + \mathcal{O}(Q^4)\right), \\
&= (\gamma^0 E - i\gamma^k Q_k + m_\mu)\frac{1}{2}\left(\frac{1}{m_\mu} - \frac{1}{2!}\frac{Q^2}{m_\mu^3} + \mathcal{O}(Q^4)\right), \\
\bar{u}(s')\frac{-iQ'^{+} + m_\mu}{2E} &= \bar{u}(s')(\gamma^0 E - (i+1)\gamma^k Q_k + m_\mu)\frac{1}{2}\left(\frac{1}{m_\mu} - \frac{1}{2!}\frac{Q^2}{m_\mu^3} + \mathcal{O}(Q^4)\right), \\
&= \bar{u}(s')(2m_\mu - (i+1)\gamma^k Q_k)\frac{1}{2}\left(\frac{1}{m_\mu} - \frac{1}{2!}\frac{Q^2}{m_\mu^3} + \mathcal{O}(Q^4)\right), \\
\Rightarrow \bar{u}(s')f'^{+}(Q) &= \bar{u}(s') + \mathcal{O}(Q),
\end{aligned}
\tag{4.128}
$$

where in going to the penultimate line, we used Equation 4.98. We note the $\mathcal{O}(Q)$ terms will vanish since the final expression is evaluated at $Q = 0$. We get a similar term for $f^-(Q)u(s)$:

$$
u(s)f'^{-}(Q) = u(s) + \mathcal{O}(Q). \tag{4.129}
$$

Finally, we can put all the terms together and evaluate at $Q = 0$, giving us

$$
\bar{u}(s')\frac{\partial}{\partial Q_i}\mathcal{M}_\nu(Q)\bigg|_{Q=0} u(s) = -\bar{u}(s')\left(\frac{iS^{i\nu}}{2m}F_2(0)\right)u(s) \tag{4.130}
$$

Specialising in the spatial component, $\nu = j$, we introduce the expression for $\mathcal{M}_\nu$ into Equation 4.130,

$$
i\bar{u}(s')\sum_r \sum_{z,x_{\text{op}}} \mathcal{F}_j^c(0)\, x_{\text{op},i} u(s) = -\bar{u}(s')\left(\frac{iS^{ij}}{2m}F_2(0)\right)u(s). \tag{4.131}
$$

Multiplying Equation 4.131 by $\frac{1}{2}\epsilon_{ijk}$, we get a vector equation

$$
\begin{aligned}
\frac{1}{2}\bar{u}(s')\sum_r \sum_{z,x_{\text{op}}} i\mathcal{F}_j^c(0)\,\epsilon_{ijk} x_{\text{op},i} u(s) &= -\frac{1}{2}\bar{u}(s')\left(\epsilon_{ijk}\frac{iS^{ij}}{2m}F_2(0)\right)u(s), \\
&= \frac{F_2(0)}{2m}\bar{u}(s')\Sigma_k u(s), \\
\frac{1}{2}\sum_{r,z,x_{\text{op}}} \vec{x}_{\text{op}} \times i\bar{u}(s')\vec{\mathcal{F}}^c(0)u(s)\,\epsilon_{ijk} &= \frac{F_2(0)}{2m}\bar{u}(s')\vec{\Sigma}u(s),
\end{aligned}
\tag{4.132}
$$

where $\Sigma_k = \frac{1}{4i}\epsilon_{ijk}[\gamma^i, \gamma^j]$. We also note that the term $i\mathcal{F}^c(0)$ is equivalent to the quantum mechanical current. Indeed, the l.h.s of Equation 4.132 has the same form as a magnetic moment, μ, produced by a static (time-independent), localised current, $J(r)$. In the continuum form,

$$\vec{\mu} = \frac{1}{2}\int d^3r\, \vec{r} \times \vec{J}(\vec{r}), \tag{4.133}$$

where $\vec{\mu}$ is the magnetic moment vector, $\vec{r}$ is the position vector and $\vec{J}(\vec{r})$ is the classical electric current. For the details regarding the relation between Equation 4.133 and 4.132, we refer to [18].

The $\vec{x}_{\text{op}} \times i\bar{u}(s')\vec{\mathcal{F}}^c(0)u(s)$ is the sought after expression, known as the (spatial) moment of the Feynman amplitude. When we trace back the derivation, we note that this expression originates from the matrix element of the electromagnetic current, for example see Equation 4.115 and 4.122. As mentioned in the paragraph below Equation 4.122, the presence of the Feynman amplitude $\mathcal{F}_\nu$ allows us to study the HLbL contributions at finite, albeit large volume on the lattice with small corrections, thereby circumventing the problem of taking $L \to \infty$.

Since the HLbL scattering contribution cannot be related to experimental data, alternative approaches to compute a_μ^{HLbL} are model-dependent [31]. Usually, they depend on theoretical parameters such as the smallness of chiral symmetry breaking or the large number of colour charges, N_c [31]. For example, Melnikov and Vainshtein in 2004 considered contributions parametrised by N_c, producing a value of $a_\mu^{\text{HLbL}} = (136 \pm 25) \times 10^{-11}$, where the uncertainty is subjective to estimations of the pseudoscalar and pseudovector exchanges [31]. For completeness, the model-independent HLbL contribution introduced by Blum *et al.* in 2015 gives

$$a_\mu^{\text{HLbL}} = (132.1 \pm 6.8) \times 10^{-11} \text{ [18]}. \tag{4.134}$$

5 Conclusion

The anomalous muon magnetic moment, a_μ, is defined as the deviation from the Dirac moment [6]. This effect is due to radiative and higher order loop corrections. As such, the anomalous muon magnetic moment serves as an excellent low energy probe for new physics [4], which appears as a discrepancy between the experimentally measured a_μ to that predicted by the Standard Model. The measurements made at the Brookhaven National Laboratory in the course of 1999 to 2001 yielded an experimental value of [4]

$$a_\mu^{\text{E821}} = 11659208.0(5.4)(3.3) \times 10^{-10}, \tag{5.1}$$

where the current experiment, E989, at Fermilab promises to increase the precision of the reuslt by four-fold [3].

The theoretical predictions must match in terms of precision with the ever-improving experimental setups. Recent progress by Aoyama *et al.* in [11] have computed QED contributions to a_μ^{SM} up to the tenth order and Gnendiger *et al.* [14] have completed the EW contributions up to two loops. Together, the QED and EW contributions yield

$$\begin{aligned} a_\mu^{\text{QED}} &= 116584718951(80) \times 10^{-14}\ [11] \quad (2017), \\ a_\mu^{\text{EW}} &= (153.6 \pm 1.0) \times 10^{-11}\ [14] \quad (2017) \end{aligned} \tag{5.2}$$

where the uncertainty in QED contributions come from measurement of the Rydberg constant [11] and the EW contributions come from three-loop and hadronic contributions [14].

While the QED contributions are dominant in a_μ^{SM}, the main theoretical uncertainty originates from hadronic contributions. This literature review focusses on the two hadronic contributions - the hadronic vacuum polarisation and the hadronic light-by-light scattering processes - and the numerical techniques applied in lattice QCD to evaluate them.

The hadronic vacuum polsarisation makes its contribution to a_μ^{had} via Equation 4.23. The main challenge of evaluating Equation 4.23 on the lattice is due the need for large lattice dimensions at $\mathcal{O}(10\text{fm})$, which is much too expensive for current computational resources. To this end, we explored two methods. The first is in switching the kernel function in Equation 4.23 into its time-momentum representation, $\tilde{K}(t; m_\mu)$. This gives us an explicit expression for the kernel function with an accuracy up to $\mathcal{O}(10^{-6})$. Another strategy to evaluate Equation 4.23 is to find an expression for the once subtracted vacuum polarisation function, $\hat{\Pi}(Q^2)$. The key insight proposed by Della Morte *et al.* in [17] is a hybrid strategy, where one can use the time moments as coefficients for the Padé approximants to determine $\hat{\Pi}(Q^2)$ at low Q^2. The hadronic vacuum polarisation contribution to a_μ^{had} due to the up, down, strange and charm quarks in time-momentum representation (TMR) and the hybrid strategy are summarised below [17]

$$\begin{aligned} a_\mu^{\text{HVP,TMR}} &= (616.7 \pm 24.8 \pm 28.9) \times 10^{-10}, \\ a_\mu^{\text{HVP,hybrid}} &= (623.1 \pm 25.4 \pm 19.7) \times 10^{-10}, \end{aligned} \tag{5.3}$$

where the first uncertainty is due to statistical error and the second is due to systematic error.

In principle,the contributions due to hadronic light-by-light scattering processes can be evaluated on the lattice using Equation 4.109. However, this is computationally expensive and alternative methods are used instead. The first explored in this review looks for a new method to introduce stochastic effects. This involves exploiting the translation covariance of the Feynman amplitude to shift its spacetime arguments by an average value that we can set. The second method involves deriving an expression for the amplitude moments and using it

to compute the form factor, $F_2(0)$ on the lattice. The symmetry of the setup is such that the total amplitude receives most of the contribution at the origin of the lattice and becomes exponentially suppressed in the limit of infinite volume. Below, we quote the HLbL contribution to a_μ according to Blum [18]

$$a_\mu^{\mathrm{HLbL}} = (132.1 \pm 6.8) \times 10^{-11} \quad (2015), \tag{5.4}$$

where the uncertainty quoted is due to statistical errors.

The discrepancy between the experimentally measured and theoretically predicted values of a_μ currently stands at 3.6σ [1]. It is clear from Aoyama's work [11] that while higher order corrections can reduce $a_\mu^{\mathrm{exp}} - a_\mu^{\mathrm{SM}}$, improving the precision of hadronic contributions to a_μ^{SM} will provide the final say as to whether this discrepancy is an indication of new physics or otherwise.

References

[1] F. Jegerlehner and A. Nyffeler, "The Muon g-2," *Phys. Rept.*, vol. 477, pp. 1–110, 2009.

[2] A. Hoecker and W. Marciano, "The Muon Anomalous Magnetic Moment," *Rept. Prog. Phys*, vol. 70, p. 795, 2007.

[3] I. Logashenko *et al.*, "The Measurement of the Anomalous Magnetic Moment of the Muon at Fermilab," *Journal of Physical and Chemical Reference Data*, vol. 44, no. 3, p. 031211, 2015. https://doi.org/10.1063/1.4917553.

[4] J. P. Miller, E. de Rafael, and B. L. Roberts, "Muon (g-2): Experiment and Theory," *Rept. Prog. Phys.*, vol. 70, p. 795, 2007.

[5] T. E. Phipps and J. B. Taylor, "The Magnetic Moment of the Hydrogen Atom," *Phys. Rev.*, vol. 29, pp. 309–320, Feb 1927. https://link.aps.org/doi/10.1103/PhysRev.29.309.

[6] A. Zee, *Quantum Field Theory in a Nutshell*. Nutshell Handbook, Princeton, NJ: Princeton Univ. Press, 2003.

[7] G. W. Bennett *et al.*, "Final Report of the Muon E821 Anomalous Magnetic Moment Measurement at BNL," *Phys. Rev.*, vol. D73, p. 072003, 2006.

[8] C. E. Thomas, "The Standard Model." Mathematical Tripos Lent Lecture Notes, 2018.

[9] W. Liu *et al.*, "High Precision Measurements of the Ground State Hyperfine Structure Interval of Muonium and of the Muon Magnetic Moment," *Phys. Rev. Lett.*, vol. 82, pp. 711–714, Jan 1999. https://link.aps.org/doi/10.1103/PhysRevLett.82.711.

[10] C. Patrignani *et al.*, "Review of Particle Physics," *Chin. Phys.*, vol. C40, no. 10, p. 100001, 2016.

[11] T. Aoyama, M. Hayakawa, T. Kinoshita, and M. Nio, "Complete tenth-order qed contribution to the muon $g-2$," *Phys. Rev. Lett.*, vol. 109, p. 111808, Sep 2012. https://link.aps.org/doi/10.1103/PhysRevLett.109.111808.

[12] J. Schwinger, "On Quantum-Electrodynamics and the Magnetic Moment of the Electron," *Phys. Rev.*, vol. 73, pp. 416–417, Feb 1948.

[13] P. J. Mohr, B. N. Taylor, and D. B. Newell, "CODATA recommended values of the fundamental physical constants: 2010," *Reviews of Modern Physics*, vol. 84, pp. 1527–1605, Oct. 2012.

[14] C. Gnendiger, D. Stöckinger, and H. Stöckinger-Kim, "The electroweak contributions to $(g-2)_\mu$ after the higgs-boson mass measurement," *Phys. Rev. D*, vol. 88, p. 053005, Sep 2013. https://link.aps.org/doi/10.1103/PhysRevD.88.053005.

[15] J. Beringer *et al.*, "Review of Particle Physics," *Phys. Rev. D*, vol. 86, p. 010001, Jul 2012. https://link.aps.org/doi/10.1103/PhysRevD.86.010001.

[16] C. Gattringer and C. B. Lang, "Quantum Chromodynamics on the Lattice," *Lect. Notes Phys.*, vol. 788, pp. 1–343, 2010.

[17] M. Della Morte, A. Francis, V. Gülpers, G. Herdoíza, G. von Hippel, H. Horch, B. Jäger, H. B. Meyer, A. Nyffeler, and H. Wittig, "The Hadronic Vacuum Polarization Contribution to the Muon $g-2$ from Lattice QCD," *JHEP*, vol. 10, p. 020, 2017.

[18] T. Blum, N. Christ, M. Hayakawa, T. Izubuchi, L. Jin, and C. Lehner, "Lattice Calculation of Hadronic Light-by-Light Contribution to the Muon Anomalous Magnetic Moment," *Phys. Rev. D*, vol. 93, p. 014503, Jan 2016. https://link.aps.org/doi/10.1103/PhysRevD.93.014503.

[19] D. Bernecker and H. B. Meyer, "Vector Correlators in Lattice QCD: Methods and applications," *Eur. Phys. J.*, vol. A47, p. 148, 2011.

[20] E. W. Weisstein, "Modified Bessel Function of the Second Kind." http://mathworld.wolfram.com/ModifiedBesselFunctionoftheSecondKind.html. From MathWorld - A Wolfram Web Resource.

[21] E. W. Weisstein, "Laplace Transform." http://mathworld.wolfram.com/LaplaceTransform.html. From MathWorld - A Wolfram Web Resource.

[22] E. W. Weisstein, "Reflection Relation." http://mathworld.wolfram.com/ReflectionRelation.html. From MathWorld - A Wolfram Web Resource.

[23] E. W. Weisstein, "Modified Bessel Function of the First Kind." http://mathworld.wolfram.com/ModifiedBesselFunctionoftheFirstKind.html. From MathWorld - A Wolfram Web Resource.

[24] E. W. Weisstein, "Digamma Function." http://mathworld.wolfram.com/DigammaFunction.html. From MathWorld - A Wolfram Web Resource.

[25] E. W. Weisstein, "Euler-Mascheroni Constant." http://mathworld.wolfram.com/Euler-MascheroniConstant.html. From MathWorld - A Wolfram Web Resource.

[26] M. Lotz, "Padé Approximation." https://na2.org/lectures/. Numerical Analysis 2 Lecture Notes.

[27] M. Barnsley, "The bounding properties of the multipoint padé approximant to a series of stieltjes on the real line," *Journal of Mathematical Physics*, vol. 14, no. 3, pp. 299–313, 1973.

[28] J. Jackson, *Classical electrodynamics*. New York: Wiley, 1999.

[29] D. Tong, "Quantum Field Theory." Mathematical Tripos Michaelmas Lecture Notes, 2018.

[30] H. Murayama, "Quantum Field Theory II: Fermi Systems." `http://hitoshi.berkeley.edu/`. 221B Spring Lecture Notes.

[31] K. Melnikov and A. Vainshtein, "Hadronic Light-by-Light Scattering Contribution to the Muon Anomalous Magnetic Moment Reexamined," *Phys. Rev. D*, vol. 70, p. 113006, Dec 2004.